Recent advancement in solar-driven interfacial steam generation for desalination: A state-of-the-art review

Soumya Kanti Hazra[a*#], Ahmed Mortuza Saleque[b*], Amrit Kumar Thakur[c*], Md. Nahian Al Subri Ivan[d], Dipankar Biswas[e], Shahid Ali Khan[f], R. Saidur[g,h], Zhenjun Ma[i], Ravishankar Sathyamurthy[j]

[a] Cryogenic Engineering Centre, Indian Institute of Technology Kharagpur, West Bengal 721302, India

[b] Department of Electrical and Computer Engineering, University of California, Davis, CA 95616, USA

[c] Department of Mechanical Engineering, University of California, Merced, CA 95343, USA

[d] Department of Applied Physics, Photonic Research Institute and Materials Research Center, The Hong Kong Polytechnic University, Hung Hom, Kowloon, Hong Kong

[e] Department of Electronics and Communication Engineering, Institute of Engineering and Technology, GLA University, Mathura, UP 281406, India

[f] Department of Mechanical Engineering, City University of Hong Kong, Hong Kong

[g] Research Center for Nano-Materials and Energy Technology (RCNMET), School of Engineering and Technology, Sunway University, Bandar Sunway, Petaling Jaya 47500, Selangor Darul Ehan, Malaysia

[h] School of Engineering, Lancaster University, Lancaster LA1 4YW, UK

[i] Sustainable Buildings Research Centre, University of Wollongong, Wollongong, Australia

[j] Mechanical Engineering Department, King Fahd University of Petroleum and Minerals, Dhahran, Saudi Arabia

[#] Present address: Department of Mechanical Engineering, Indian Institute of Technology Patna, Bihar 801103, India

***Corresponding Authors**

Soumya Kanti Hazra – soumyakantihazra@gmail.com

Amrit Kumar Thakur – amritt1@gmail.com

Ahmed Mortuza Saleque – ahmed.saikot@gmail.com

Abstract

Solar energy is one of the most efficient origins of energy for a wide range of environmentally beneficial purposes. Water desalination by steam generation with the help of solar energy is not only economical and straightforward approach, but it also utilizes free energy sources to solve the problem of increasing freshwater scarcity. Solar water evaporation is an essential component of the low-energy method for generating fresh water, which is required for economic development and human health. Freshwater productivity determines how effectively the system captures incoming solar energy and transforms it into usable heat. Effective water distillation has recently gained a lot of attention. The photothermal conversion process is built on the performance of the evaporator. This review thoroughly examines the most recent developments in photothermal materials, structure design, and engineering strategies, including design principles for highly efficient photothermal conversion, thermal management, water transport phenomena, salt rejection behaviour, and improved evaporation rate. The prospective applications of this technique in saline water desalination, wastewater purification, and energy generation are highlighted. Furthermore, the most recent scientific advancements are utilized to demonstrate the potential, prospects, and challenges of solar-driven evaporation in energy conversion.

Keywords: solar steam generation, desalination, photothermal conversion, absorber, salt rejection

1. Introduction

The only planet with readily available oxygen and water for life is Earth. Pure drinking water is considered a universal concern, vital to the survival of humanity, economic growth, and societal advancement [1]. Many communities are facing a freshwater crisis as a result of rapid rises in the population, climate fluctuations, and increasing pollution in recent years [2,3]. Water is the utmost prevalent chemical substance on earth, covering 71% of its surface. However, for at least one month out of the year, two-thirds of the world's population experiences water scarcity [4]. Therefore, the lack of water resources is a significant challenge for the twenty-first century [5]. However, around 3% of fresh water on earth may be instantly consumed by humans for living, while only about 97% of seawater cannot drink directly [6]. By 2025, World Health Organization (WHO) projects that half of humanity will reside in areas with scarce water supplies. As a result, there is an urgent need for large-scale, effective saltwater desalination systems. Reverse osmosis [7] and multi-stage flash [8] are examples of traditional desalination methods. These technologies are thriftily and geologically infeasible for rural areas. The results from expensive infrastructure and installations, significant energy usage, and accessibility issues. Generally, traditional seawater desalination equipment requires fossil fuels to operate. For example, ten thousand tonnes of oil must be used annually to yield freshwater of 1000 m^3 per day, significantly increasing greenhouse gas emissions [9,10]. Consequently, it is critical for the production of freshwater and wastewater treatment systems driven by sustainable and clean energy [11,12].

Earth's primary energy source is solar energy, which has rewards of being fresh and regenerative. Solar energy is a promising source to fulfil future energy demands among all renewable sources [13-15]. Solar mediated water evaporation, commonly

referred to as solar steam generation (SSG), is an alternative sustainable method of producing pure water. High purity water can be created by SSG using solar irradiance and then condensing it [16-18]. Interestingly, the working temperature is substantially lower than water's boiling point in SSG system. Therefore, 90% efficiency of SSG may be easily reached since it concentrates on improving heat localization at the liquid surface [19]. Due to poor sun absorption and substantial heat losses, conventional solar evaporation methods typically have low photothermal efficiencies lie between 30 to 45%, making them an unfeasible method for producing significant amounts of clean water [20,21]. Thus, novel device designs, improved light absorbing materials, and modules for highly efficient solar steam generation techniques are required. The SSG method has numerous benefits compared to alternative methods: utilizing adequate heat for water evaporation, reducing volumetric heating. Besides, this method can purify water with minimal energy and CO_2 emissions [22].

However, natural water evaporation efficiency is significantly less to produce a useful volume of fresh water as water's weak optical absorption behaviour and severe heat losses. Through a selection of photothermal nanomaterials (PMs) and the configuration of SSG systems that promote interfacial heating, much work has been put into building enhanced SSG systems with improved efficiency [23-26]. In this technique, scheming efficient solar absorbers and integrating with different PMs to increase the amount of captured solar energy and utilization of produced heat energy. This increases the efficiency of solar evaporation by effectively absorbing the broad solar spectrum and substantially reducing heat loss to the environment. Additionally, medical sterilization or sanitization can be accomplished using solar steam generation [27-29]. This technology can be divided into two types such as direct and indirect way. In the direct process, steam is produced immediately following the direct conversion

of solar radiation into heat. In contrast, in the indirect method, solar irradiance is first transformed into electrical power, which is then utilized to generate the heat necessary for the subsequent process of creating steam [30]. Flat surfaces used in direct strategy collect incoming solar radiation, which is transformed to heat energy and causes water evaporation. Unlike indirect systems, direct systems do not involve the movement of water; instead, steam is produced right where the water is exposed to the sun [30].

Another significant source of freshwater is wastewater treatment, which is mostly produced by industry. Activated carbon adsorbents, where the active material for removal absorbs contaminants, are a commonly used method for wastewater treatment. The limitations of common adsorbent materials include incomplete elimination of hydrophilic microcontaminants, sluggish contaminants uptake, and difficulties in restoring absorbent [31]. To reduce the rising mandate for fresh water and energy consumption, it is necessary to create sophisticated, renewable, and sustainable methods for producing pure water. As a result, harvesting of pure water from numerous origins (including seawater, rivers, sewage, etc.) SSG has garnered the attention of researchers worldwide. Undoubtedly, one of the most effective methods to reduce the global water problem is solar desalination, which can employ plentiful and accessible seawater and unending sun energy to create freshwater [32,33].

Herein, the characteristics and photothermal conversion mechanism of only a particular type of materials are not covered but highlighted in almost all types (such as metallic, semiconductor, carbon-based, and polymeric). The review evaluates recent developments and analyses studies on materials and structures for solar evaporators, specifically in the SSG system. There have been numerous comprehensive assessments in the field of solar energy conversion in recent years. A summary of the

pertinent issues is presented, along with a potential roadmap for future research plan and implementation of solar driven interfacial steam generation for desalination. This paper highlights the most recent advancements in this area. Initially, the fundamental principles of photothermal conversion and notable parameters are clarified. After that, the design approach of the SSG system is scrutinised. Pivotal components for manufacturing proficient SSG comprise prompt water transportation, effortless steam release, efficient thermal management, and vapour condensation. Most recent literature reviews on solar steam generation have been primarily concerned with examining the various materials employed and their associated synthesis techniques for constructing solar absorbers and support substrates in SSG systems. These reviews feature analysis of different configurations that utilise alternative materials to enhance SSG efficiency [34-36]. As a result, this present review focuses mostly on the system's performance using various photothermal materials and overall system configuration, including the structure of the evaporator, and different materials for absorbers.

The solar steam generation process entails converting solar energy absorption into thermal energy, which drives the generation of steam. Research has primarily concentrated on different types of solar absorber materials and configurations with the aim of improving evaporation rates and enhancing desalination productivity. Very few reviews have specifically focused on issues such as salt precipitation and wastewater treatment, while the efficient vapor collection process remains relatively unexplored. The recovery of freshwater from condensed vapour is an important factor in improving the overall productivity of solar desalination. Although the initial two phases, where solar energy is transformed into thermal energy and vapor is generated by the thermal energy, have been researched, the final phase has received less attention. This review

also aims to investigate the impact of employing multiple techniques to enhance water evaporation and condensation rates in order to improve the productivity of solar steam generation-based desalination. This review provides a concise overview of various methods to increase condensation rates, such as water and air glass cooling, external condensers, and thermoelectric cooling, and their influence on the productivity. Moreover, the possibility of combining different techniques in SSG systems is explored.

The review comprises eight sections discussing techniques for evaluating the efficiency of solar evaporators, research on photothermal materials and solar evaporator structures, improvements in water transport, resistance to salt, corrosion resistance of the water transportation layer, water productivity through condensation, strategies for efficient energy use, and diverse applications. The objective of this review is to provide an overview of the performance of a range of SSG systems across diverse materials and configurations. A comprehensive evaluation of prevalent SSG applications in desalination of saline water, wastewater treatment, and energy production is presented. Challenges and key issues are addressed to enhance understanding and provide direction for future SSG developments aimed at producing clean water.

2. Solar steam generation systems

In typical SSG systems, solar energy is received, absorbed, and converted into thermal energy by a solar absorber, which is utilised to heat water to produce vapour [37]. SSG systems can be divided into two groups based on where the PM is positioned in the bulk fluid. One approach is volumetric and another is interfacial steam generation [38]. Their graphical representation is shown in Fig. 1. In the first type of

system, PM is uniformly dispersed in a bulk medium. The illustration of the volumetric system is presented in Fig. 1(a). In this system, PMs are dispersed in bulk liquid, acting as tiny absorbers [39-42]. When exposed to sunlight, temperature on the surfaces of PMs can increase quickly due to their strong photothermal conversion behaviour. At the particle-liquid interface, vapour develops and creates a thin layer of steam. Nanoparticles covered in vapour eventually travel to the liquid-air boundary under continuous sunlight, releasing the vapour and returning it to liquid. Generally, surface of nanoparticles acts as a heat source to initiate vaporisation. This method often relies on expensive optical concentrators and prolonged time to allow bulk heating of liquid. The hot bulk water's susceptibility causes low efficiency to numerous temperature fatalities and excessive heating of liquid's portion that isn't used to produce steam [43].

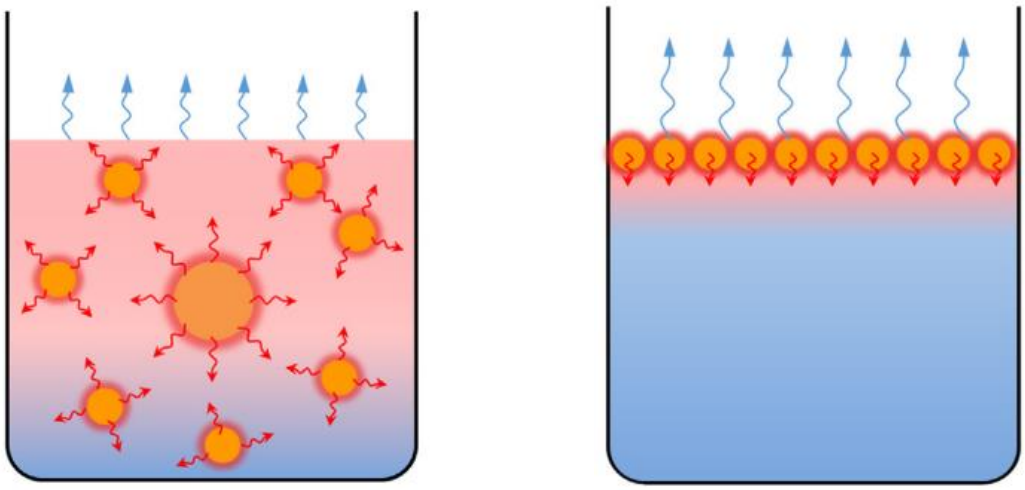

(a) **(b)**

Figure 1. Graphics of solar steam generation system (a) volumetric, (b) interfacial [44].

The second system, shown in Fig. 1(b), is an interfacial SSG system in which bulk fluid and photothermal materials are separated. Solar absorbers are used in the SSG system to localize heat generation. There are two possible positions for solar

absorbers in solar evaporation systems. Solar absorbers can be positioned at the water-air interface in one instance and at the bottom of the system in another. An illustration of different systems having different absorber positions is shown in Fig. 2.

2.1. Solar absorber fixed at the bottom

As seen in Fig. 2(a), incoming sunlight flows through water and transforms into thermal energy on solar absorbers when the absorber is positioned at the bottom. The temperature of bulk water gradually rises, hastening the evaporation of water. Based on this technique, the related investigations have built a variety of solar stills for producing water. Even under optimal operating conditions, efficiency and water production rate are very low, mostly attributable to lower absorption caused by water reflection and significant heat loss to heat bulk water [45-48].

2.2. Floating on top surface

A floating solar absorber designs an effective evaporation system on the top surface of water, as presented in Fig. 2(b). Solar irradiance falls on the absorber in this mode, where it transforms into thermal energy made from PMs. High evaporation is achieved by reducing heat loss to bulk medium and directly heating the water inside floating absorbers using the located thermal energy [49-52].

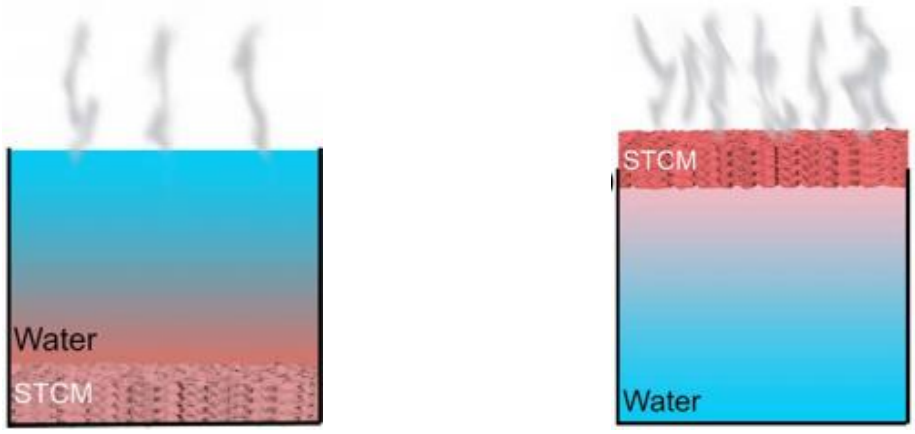

(a) **(b)**

Figure 2. Schematic of solar steam generation system based on absorber position at (a) bottom, (b) top surface [53].

The solar absorber and supporting substrate layer are two primary parts of the nanostructured interfacial solar vapour generator. Absorbers should be proficient in capturing a lot of solar energy and have a weak natural tendency to reflect and transmit electromagnetic waves. A high solar absorption capacity greatly improves photothermal conversion efficiency and significantly lowers radiation heat losses due to transmission and reflection. The floating porous layer serves as the supporting substrate layer and thermal insulation. The porous layer only allows underlying bulk water to be transported to the air-water interface via porous structure and reduces the conduction heat loss to bulk water [54]. Hence, it must be microporous, have good hydrophilicity, be durable, be light in weight, and have low thermal conductivity. SSG can be improved in several ways: first, by producing solar absorbers with superior photothermal conversion capabilities; second, by using supporting substrates with a suitable route for water transportation; and third, by improving thermal management to reduce heat losses from the absorber.

3. Estimation of the system performance,

Specific water productivity (WP), the quantity of water obtained per unit area of solar radiation received over a given period, is the most pertinent parameter for assessing the effectiveness of the SSG system for desalination. This parameter is considered a primary performance indicator [55,56]. The water production rate can be computed as the following given solar irradiation (G), solar energy consumption efficiency for

evaporation (η_{eva}), and specific energy consumption (EC) for the generation of a unit volume of water. Specific water productivity (WP) can be written as

$$\mathrm{WP} = \frac{\mathrm{G}\eta_{eva}}{\mathrm{EC}} \tag{1}$$

In this case, water evaporates in two stages: one employs solar absorbers to convert solar to thermal energy, and the other evaporates water using thermal energy. The absorber's solar absorbtivity (a) can be used to measure photothermal conversion efficiency in the first stage. We denoted thermal efficiency of evaporation as η_{TE}. Consequently, solar energy consumption efficiency for evaporation can be represented as

$$\eta_{eva} = \mathrm{a}\eta_{TE} \tag{2}$$

Besides, WP is determined in an SSG by Gained output ratio (GOR) and the specific latent heat (L) of water evaporation. GOR measures the proportion of heat production utilized for evaporation and is quantified by the amount of latent heat of condensation used for distillation [57]. Gained output ratio is calculated as the kilogramme of distilled water generated per kilogramme of vapour created. Therefore, specific energy consumption (EC) for the generation of a unit volume of water can be written as

$$\mathrm{EC} = \frac{\mathrm{L}}{\mathrm{GOR}} \tag{3}$$

Finally, equation (1) can be written using equations (2) and (3) as [58]

$$\mathrm{WP} = \frac{\mathrm{G}}{\mathrm{L}}\mathrm{a}\eta_{\mathrm{TE}}\mathrm{GOR} \tag{4}$$

Since equation (4) holds true for all SSG systems, independent of the particular system architecture, this equation is crucial because it precisely comprehends how enhancing the efficiency of three essential conversion processes can improve the

overall performance of the system and their graphical presentation is shown in Fig. 3. The first process turns solar radiation into heat, the second process uses heat to create steam, and the third process changes vapour into water. The analysis indicates that solar-thermal energy may have limitations in producing vapor due to parasitic heat losses, reducing thermal efficiency for vapor generation. Besides, equation (4) demonstrates the potential for enhancing WP by increasing the GOR. This ratio provides an estimate of the frequency with which latent heat is reused. A well-thermally insulated SSG desalination system should ideally have a GOR greater than one.

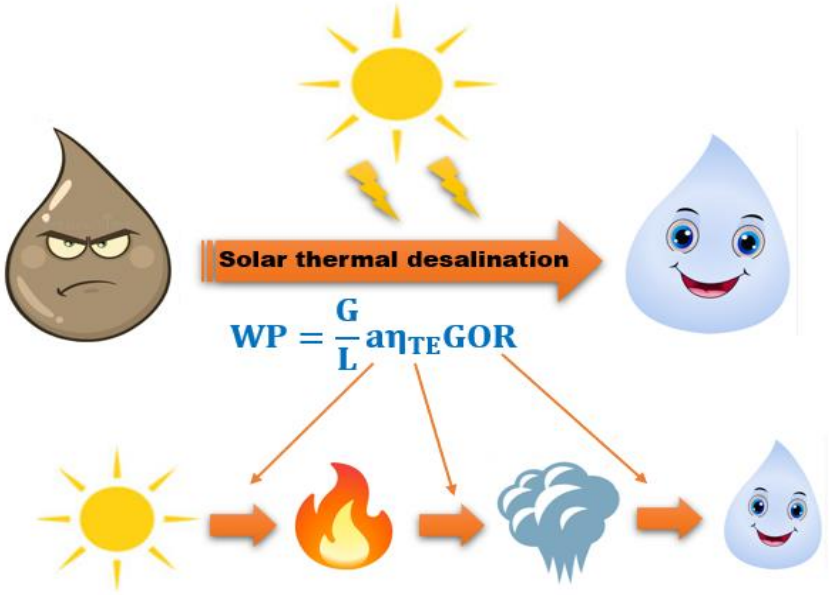

Figure 3. Schematic of solar thermal desalination process and the diagram inspired from [58].

4. Development of solar-driven interfacial evaporation systems

4.1. Characteristics and mechanism of photothermal materials

The recent advances in nanotechnology provide numerous methods of creating functional nanomaterials for energy conversion. Tailored nanomaterials with superior

optical properties are essential to intensify harvesting of solar energy and transform energy into thermal energy. Various nanomaterials are constantly being researched in order to suit the exact application requirements and achieve high efficiency in SSG systems [59]. Solar radiation can be efficiently collected by the layer of PMs of an evaporator, transforming solar energy into thermal energy. Generally speaking, an excellent photothermal material needs to possess the following [60].

- Solar absorbers can efficiently absorb light from the entire solar spectrum to make the most of solar energy irradiation.
- Solar absorbers efficiently convert light energy into heat energy without converting it to other energy or radiating it.
- Limiting thermal losses from absorber to ambient and bulk water and heat generated can be transmitted efficiently for vaporisation.
- Qualities in the substrate material design for sufficient passage for water transfer and acts as a thermal barrier.

The solar energy that reaches the earth has spectral wavelengths between 150 and 4000 nm. The visible spectrum region of solar radiation is between wavelengths of 400 and 760 nm, the infrared spectrum region is between wavelengths of 760 and above, and the ultraviolet spectrum region is between wavelengths of less than 400 nm. Solar spectrum's peak energy around 475 nm is mainly in the visible range. Yet, for effective solar absorbers, it's crucial that materials don't solely absorb within this range but instead capture a broad spectrum from 250 to 2500 nm. Research shows this broader absorption is more efficient in generating thermal energy [61,62]. Plasmonic materials, with narrow absorption peaks in visible wavelengths, might miss capturing diverse sunlight. In contrast, carbon-based materials, with their broadband absorption, are more efficient at converting solar energy into thermal energy [63].

Various materials such as metallic, semiconductor, carbon-based, and polymeric materials are the most common PMs utilised in evaporators of SSG systems.

4.1.1. Metallic nanoparticles

The mechanism for photothermal conversion (PTC) of metallic nanoparticles (NP) is a photothermal effect of localised surface plasmon resonance (SPR) [64]. While big metallic nanoparticles primarily scatter light, small metallic NPs absorb light. A photothermal effect occurs when metallic nanoparticles absorb or scatter photon energy, with most of the absorbed energy being emitted as heat [65]. Au, Ag, Cu, etc., have excellent light-absorbing properties [66]. A schematic representation of SPR phenomena is presented in Fig. 4(a).

Although Au NPs are costly, they are still frequently utilised to support other photothermal materials. Zhu et al. [56] decorated Au NPs on wood to create plasmonic wood, and plasmonic wood had significant absorption (~100%) behaviour compared to the original sample. Gao et al. [28] mixed Au in a nanoporous silica matrix to fabricate a solar absorber. In the absorber, silica gel served as an insulating material to prevent heat loss; Au provided SPR for efficient solar absorption followed by significant heat in the system. Up to 85% of high evaporation efficiency was seen. Additionally, it was discovered that the diameter and shape of the Au might have a big impact on photothermal conversion. Similarly, Wang et al. [67] decorate Au and Pt NPs on titanium dioxide to increase the composite material's capacity for photothermal conversion using the SPR effect. Guo et al. [68] employed Au NPs under varying diameters ranging from 3 to 40 nm to produce solar steam. The study found that increasing the diameter of the Au NPs increased the photothermal efficiency, with samples with smaller Au having a photothermal efficiency of about 11% and samples

with larger Au NPs having a photothermal efficiency of 30%. Zhang et al. [69] decorated Au NPs decorated on rGO and attained solar 95% solar absorption capacity from the sample. Besides, Chen et al. [70] found that Au/Ag hybrid nanofluids showed higher photothermal conversion efficiency than ZnO and TiO2 nanofluids. This is because Au and Ag have separate wavebands, making it easier to match the solar spectral strength than with just one waveband. NP size may also impact the efficiency of PTC of nanofluids. According to the literature, nanofluid PTC efficiency declined when Au NP size increased. Zhu et al. [71] observed increased efficiency of seawater evaporation using Au NPs and obtained superior thermal and chemical stability even at 500 °C. To produce effective SSG, Lin et al. [72] coated Cu NPs on cellulose based absorber. Using Cu NPs, they achieved a 73% SSG efficiency and a reduction in surface reflection was also observed. Cu nanoparticles in the shape of cauliflower were created by Fan et al. [73] to absorb light and increase evaporation efficiency from 30 to 60%. Cu NPs were created by Xu et al. [74], implanted in a graphene matrix, and obtained around 99% absorption in the 300–1800 nm spectral range of the solar spectrum. It is reported that the size and shape of PMs can be used to adjust between absorption and scattering behaviour, which can substantially impact the PTC efficiency [75].

Comparatively less expensive than Au are aluminium (Al) nanoparticles and silver (Ag). Zhou et al. [76] used an Al NPs based 3D porous absorber that can absorb 96% in visible and near-infrared regions. Sun et al. [77] initially treated surface of Ag NPs with Poly (sodium-p-styrenesulfonate) to prevent salt buildup during SSG. They dissolved pre-treated Ag NPs in agarose gel and observed enhanced optical absorption behaviour through wavelength range of solar spectrum. Generally, PMs

that received assistance from metallic nanoparticles also successfully increased photothermal conversion.

4.1.2. Semiconductor materials

A semiconductor is electrically more conductible than an insulator. Usually, it is transparent to infrared (IR) light and opaque to visible light. Their bandgap, about 2-4 eV for organic semiconductors and 1-2 eV for inorganic semiconductors, significantly impacts absorption behaviour in visible wavelength regime. A sample's structure and chemical composition can be altered via doping or creating disorder. Therefore, characteristics of valence and conduction bands are enhanced, and PTC efficiency can be altered to narrow band gap [78]. Larger absorption spectra and high photon-harvesting efficiency are typical characteristics of semiconductors with smaller bandgaps, which improve photothermal conversion efficiency [79]. Semiconductors like black TiO_x, MoO_x are thought to be efficient photothermal evaporation materials in addition to being stable. As a result, they are frequently utilised as filers in matrices (such as polymeric and ceramic) for SSG systems [80]. A graphical representation of bandgap structures of different types of semiconductors and their optical absorption is presented in Fig. 4(b).

Wu et al. [81] obtained 92% absorption behaviour using CuS NPs-based aerogel when exposed to light with wavelengths between 290 and 1400 nm. The aerogel's absorption rate increased when it was moistened with water. Bi2S3 and nylon were utilised by Wang et al. [82] as the photothermal layer, and their PM demonstrated a 92% absorption of light for wavelengths between 300 and 900 nm. Using a black TiO_2 coated galvanised steel mesh as an absorber, Tudu et al. [83] achieved a 76% efficiency in the evaporation of seawater. The absorber demonstrated a good amount

of pure water production rate and strong self-cleaning ability during operation. Zada et al. [84] obtained 78% SSG efficiency by employing various diameters of black TiO_2 as PM in an absorber. In their investigation, Ren et al. [85] used carbonised wood adorned with TiO_2 and TiN nanoparticles for SSG and captured 98% of the solar energy. Reduced TiO_2 was produced by Ye et al. [86] and coated with stainless steel mesh for the SSG system. Under one sun (OS), they achieved a 50% conversion efficiency. Carbon-loaded porous TiO_2 foam was created by Wang et al. [87] using both carbon and TiO_2. The photothermal conversion efficiency of this system was 60%. To increase the capacity for light absorption, Sun et al. [88] combined TiO_2, SiO_2, and TiN NPs with cellulose hydrogel. They achieved 99% hydrogel absorption behaviour between 250 and 3000 nm of wavelength. Additionally, it has been claimed that prepared hydrogel can successfully filter out water contaminants. Zhang et al. [89] used TiN NPs as a solar energy converter and an absorber on a PVDF membrane, which led to a solar efficiency improvement of 65%.

4.1.3. Carbon based materials

Near infrared light can be effectively absorbed by carbon-based materials. Gao et al. [90] reported that these types of materials would experience a conjugation effect when exposed to sunlight, followed by modification in electron density inside bond; as a result, interatomic interactions take place. A hyperconjugation effect is produced when C-H, C-C bond electrons interrelate with non-bonding p orbitals or anti-bonding π orbitals [91]. When incident light energy encounters the need for the electron transition, π electrons in bonding orbital transition to π anti-bonding orbital in π-π system, which has biggest conjugation consequence in carbon-based materials. To perform a photothermal conversion, the excited electrons must return from a higher energy state to a ground energy state, emitting heat and lattice vibration. This causes

a temperature rise in carbon-based materials [92], as shown in Fig. 4(c). An ideal photothermal converter is a substance that can capture the entire solar spectrum while reflecting nothing. For better light absorbers in SSG, carbon-based PMs, including carbon nanotubes, graphene, graphene oxide, carbon black, carbonised samples, etc., are promising possibilities.

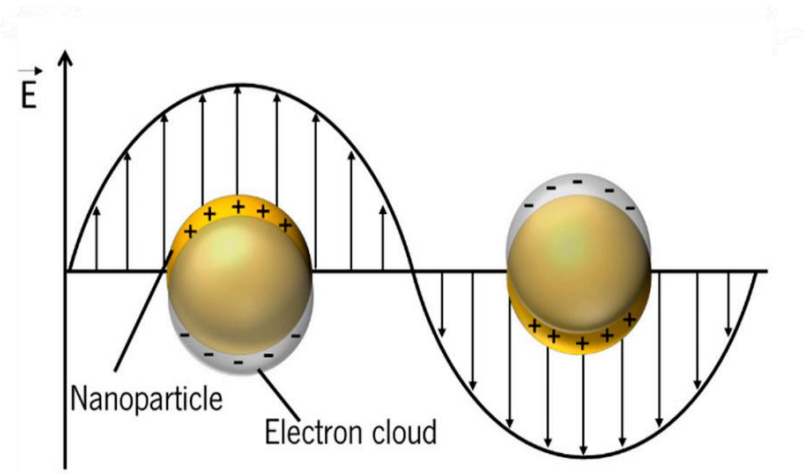

(a)

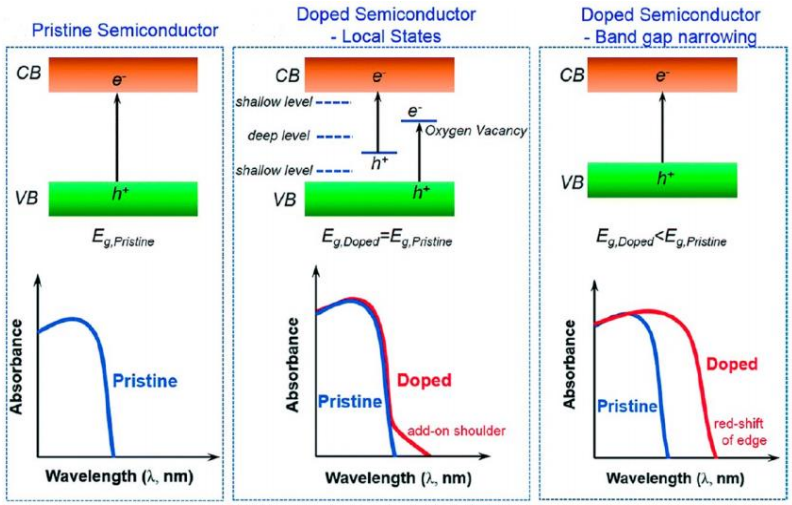

(b)

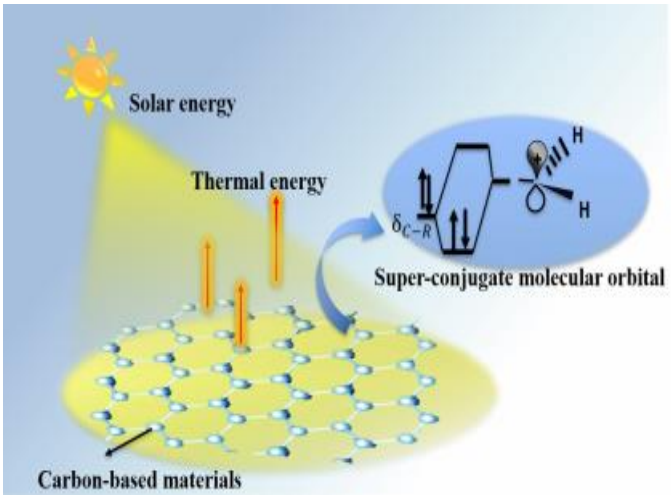

(c)

Figure 4. A graphical representation of (a) surface plasmon resonance in metals [93], (b) bandgap engineering of semiconductors and band structure vs. optical absorption of different types semiconductor material [94], (c) photothermal conversion in carbon-based material [95].

The graphene oxide/ZnO-based absorber was created by Wang et al. [96], who also measured a 91% efficiency for solar energy conversion. Hu et al. [97] suggested using aerogels with graphene oxide to improve absorption behaviour in the setup. They reported 83% efficiency under one sun and outstanding solar spectrum absorption between 200 and 500 nm. Ren et al. [33] employed graphene foam as the solar absorber in their SSG system, achieving an efficiency of about 92%. Additionally, they claimed that their absorber could capture solar radiation at any angle, minimising light reflection. Li et al. [98] looked into the impact of graphene sheet thickness on the rate of SSG evaporation. Using a 50 m film thickness, they could reach 90% efficiency in the study. Zhou et al. [99] used a combination of graphene and cellulose-made absorber to achieve a 2 kg m^2 h^{-1} evaporation rate under OS.

Additionally, they observed the absorber's improved salt rejection behaviour. 3D graphene networks and pieces of wood were suggested by Kim et al. [100] as a high

solar absorber for SSG systems. They attained a maximum conversion efficiency of 92% under light from one sun. Zhang et al. [101] found that a sponge coated with modified graphitic carbon in polydimethylsiloxane had a 74% evaporation efficiency.

4.1.4. Polymeric materials

Polymeric materials have a PTC procedure that is comparable to carbon-based particles. When excited electrons move from the lowest vacant orbital to the highest occupied orbital, they emit heat. Through lattice thermal vibration, polymeric materials achieve photothermal conversion [102]. Several groups, like hydroxyl, carboxylic, amino, sulfonic acid, etc., are commonly found in polymer chains, allowing non-covalent association with water by a hydrogen bond. To reduce the amount of energy needed for evaporation and water condition has been adjusted using chitosan. Chitosan's amino groups coexisting enhanced the intermediate water amount, facilitating water evaporation [103]. In addition to having good elasticity, calm moldability, broadband absorption, and biocompatibility for prolonged use compared to other materials, polymeric materials are also suitable for usage. Like carbon materials, polymers' photothermal conversion method hangs on molecules’ thermal vibration.

Zhang et al. [23] created an absorber using PPy coated stainless steel mesh to increase conversion efficiency. Compared to bare mesh, they saw an improvement of 24% to 58% with the addition of the PPy layer. Arginine doped polydopamine and pure polydopamine coating on wood was employed by Zou et al. [104] to study photothermal conversion behaviour. Under one sun, they achieved a 77% steam generating efficiency using doped coating. The authors observed superior optical absorption behaviour, and the conversion efficiency of doped costing is superior to

pure polydopamine coating. Polydopamine’s (PDA's) photothermal properties were studied by Wu et al. [105] using wood as a substrate for SSG, and solar evaporator could produce solar steam after 5 seconds of light exposure, and photothermal efficiency increased to 87%. Wang et al. [82] used polystyrene foam in the SSG system. Foam acted as a supporting layer and passage for water transportation. Zhao et al. created the PDA/MXene microsphere photothermal layer [106], which also combined it with wide-spectrum solar absorption capabilities. The system also allows for rapid water transfer and vapour evaporation. Under solar light from one sun, the manufactured photothermal absorber had a photothermal conversion efficiency of 86%. Huang et al. [107] polymeric sponge made of melamine due to its high porosity and water absorption behaviour. Fan et al. [108] used polysulfone-based materials to support the photothermal layer, a thermal barrier between bulk fluid and absorber.

There haven't been many studies on polymeric materials for SSG, despite their excellent broadband light absorption and the ability to bond with water to speed up evaporation. This might be caused by the utilised plasmonic nanoparticle's chemical instability, heat, etc. In order to solve the primary difficulties in locating stable polymeric materials that are simple and affordable to scale up, more research is necessary.

4.1.5. Comparison of solar evaporator materials

Metallic nanoparticles heat up quickly and have the best photothermal conversion impact in the evaporator's photothermal layer. However, they are unsuited for large production or long-term use because of their high cost, low stability, and ease of oxidation. Semiconductors are adaptable and inexpensive, but their reprocessing is challenging and has poor stability in practical applications. For SSG systems, polymeric materials have strong biocompatibility. On the other hand, carbon-based

materials have many benefits, including affordability and stability. Carbon based materials can absorb the whole spectrum of sun wavelengths. High-quality carbon-based products shouldn't be produced in large quantities. A more environmentally friendly method of generating porous carbon materials is required to improve water transportation as well as steam production in PTC applications. Polymeric materials make an effective thermal insulating water transport layer for evaporators because of their distinctive porosity structure, low thermal conductivity, and inexpensive cost.

4.2. Structures of a solar evaporator

An effective solar evaporator has two main functions, i) Absorbing a broad spectrum of light at the solar absorbing surface and converting them to heat, ii) Absorbing water and transferring them to the place where heat is localized. Over the years, various types of structures have been developed to facilitate those two functions. In most cases, photothermal materials are deposited or grown on top of a supporting substrate. For efficient solar evaporation, the supporting substrate must have the capability to transport water and reduce heat loss [109]. Depending on the thickness, the structure of the solar evaporator can be classified as a 2D structure and a 3D structure. The 2D structures are basically made of different types of membranes [109-111], paper [112,113], and fabrics [114,115], whereas 3D structures are fabricated using different types of foams, hydrogel or aerogel, bio-derived materials (i.e., wood).

4.2.1. Two dimensional structure

The solar evaporator with two dimensional (2D) structure is thin and sometimes supported by a base to keep them floating on water. Either depositing photothermal materials generally fabricate these types of solar evaporators on the top of a thin substrate or by fabricating thin solar absorbing membranes directly incorporating

photothermal materials. PTFE (Polytetrafluoroethylene) membrane is one of the most commonly used substrates for fabricating 2D solar evaporators. Chang et al. [111] fabricated a solar evaporator by forming a thin layer of hydrophobic $W_{18}O_{49}$ mesocrystal on a hydrophilic PTFE membrane substate using flow through the method, which evaporates water at 82% efficiency under OS. PTFE membrane is suitable for making solar evaporators due to its high temperature resistance, mechanical strength, stability, flexibility, and anti-acid-base property [3]. Filtration methods are one of the most used techniques to decorate photothermal materials on membranes. The use of polydopamine (pDA) is also common in such types of evaporators. Functionalized (catechol and amine group) pDA coating can make the solar evaporator hydrophilic [116]. Hydrophobic PTFE membranes are also used to make solar evaporators by vacuum filtration [117,118]. Cheng et al. [113] utilized a vacuum filtration method to fabricate rGO composite membrane using filter paper (as shown in Fig. 5(a)) and developed a system using membrane which showed a 1.37 kg m^{-2} h^{-1} evaporation rate and 85.6% efficiency under OS. Guo et al. [114] utilized spin coating method to load the filter paper with CNT based solution and sprayed polyurethane foam, and solidified it on the membrane to make an integrated evaporation device that exhibited maximum PTC efficiency of 88% under OS.

Cotton fabric is another suitable substrate for making 2D evaporators due to its stability and hydrophilicity. Li et al. [117] prepared a fabric having tuneable water delivery (TWD) property by electrospray PVDF-HFP (as shown in Fig. 5(c)) and later on fabricated a solar evaporator by dip-coating prepared TWD fabric with carbon black (PM) dispersion which shows vapour conversion efficiency of 90% with an evaporation rate of 1.33 kg m^{-2} h^{-1}. During the evaporation experiment, the thin TWD fabric based solar evaporator was placed on a cotton fabric supported by a PS foam to keep it

floating on water [115], as shown in Fig. 5(c). Such use of support foam to make thin solar evaporators float on water is a very common technique. However, keeping the evaporator floating on top of the water is not the only function of PS foam. PS foam is also utilized to keep the photothermal conversion layer separate from bulk water to reduce heat dissipation [113].

Lu et al. [118] loaded molybdenum oxides hierarchical nanostructure on hydrophilic PTFE membrane to make a solar evaporator that shows an evaporation rate and efficiency of 1.26 kg m^{-2} h^{-1} and 86% respectively under OS. Huang et al. [119] spray-coated PTFE film with MoS_2/LaF_3/PDMS to fabricate a solar evaporator, which showed a water evaporation rate and efficiency of 1.8 kg m^{-2} h^{-1} and 91% respectively. Polyvinylidene fluoride (PVDF) is another important component for making membrane based 2D solar evaporators [111,120-124]. PVDF fibre membrane has good thermal stability, low thermal conductivity, excellent mechanical strength and chemical resistance [124]. Photothermal materials can either be directly deposited on PVDF filter membrane by filtration [111] or mixed with PVDF solution to make a membrane [121]. The electrospinning method is another way to make 2D solar evaporator based on PVDF membrane. Whereas, Huang et al. [125] fabricated PDMS/CNT/PVDF membrane (productivity 1.43 kg m^{-2} h^{-1}) by forming the bottom PVDF layer by electrospinning and the middle CNT layer by spraying and top PDMS layer by soaking in PDMS solution (as shown in Fig. 5(d)). Tessema et al. [126] made a solution using Cs_xWO_3@g-C_3N_4, DMF and PVDF and spun into fibre membranes (water evaporation efficiency of 95.4%). Gao et al. [127] prepared a cheap solar evaporator (cost less than $1 per m^2) by capturing candle soot from wet cotton fabric. Qin et al. [128] fabricated a janus hybrid system for solar steam generation by dip coating cotton cloth with carbonized carrot powder dispersion and dropping Nafion, which exhibited 1.88

kg m^{-2} h^{-1} and 1.52 kg m^{-2} h^{-1} evaporation rate for pure water and sea water under OS. A thin solar evaporator can also be fabricated using a paper substrate. Shan et al. [129] constructed CTGS/Paper by attaching CTGS film on the surface of commercial A4 printing paper, which exhibits an evaporation rate and efficiency of 1.53 kg m^{-2} h^{-1} and 96% under OS. Qi et al. [115] fabricated multi-layer MWCNTs-COOH/BN-PDA/CF utilizing cotton fabric and PS foam as supportive solid, SSG shows a 1.60 kg m^{-2} h^{-1} evaporation rate under OS. Chen et al. [116] used activated carbon cloth to synthesize $NiFe_2O_4$-NiAl-LDH-ACC by hydrothermal method. They demonstrated its application in solar steam generation. Except for these many other thin solar evaporators (i.e., activated pulverised coal-based membrane (APC) derived from activated pulverised coal and filter membrane [128], self-assembled Fe_3O_4@C film [129], rGO/PS@PSf and CB/rGO/PS@PSf fabricated by coating rGO/PS and CB/rGO/PS microspheres on polysulfone (PSf) membrane [109]) can also be categorised as a 2D structured evaporator.

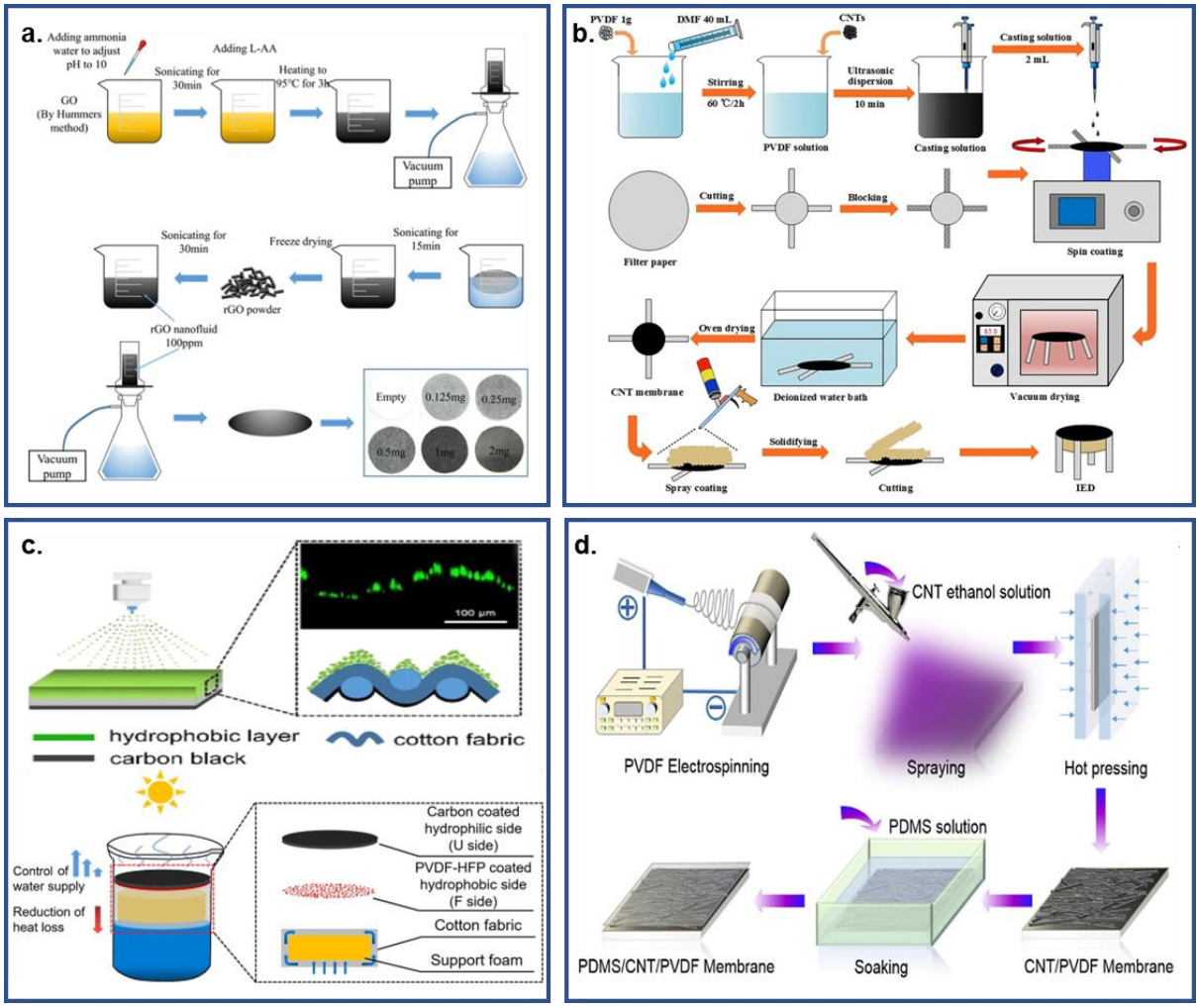

Figure 5. Fabrication process of 2D solar evaporators (a) vacuum filtration to decorate photothermal materials on filter paper [112], (b) decorating filter paper with photothermal material by spin coating [113], (c) electrospray on cotton fabric with PVDF-HFP to make a fabric with tuneable water delivery property [115], (d) fabrication of PVDF membrane by electrospinning [123].

4.2.2. Three dimensional structure

The evaporators with three dimensional (3D) structures are comparatively thicker. The substrates used for 3D structured evaporators are porous and have the capability of water transport by capillary action. The thick substrate of porous 3D structure has the capability of trapping light, storing heat and reducing heat loss, making them very

suitable for designing interfacial solar steam generation. Generally, different types of woods, foams, sponges, gels, etc., are used as substrates for making 3D structures. Wood is very suitable for making sustainable solar evaporators as it has a naturally porous structure and can absorb and transport water by capillary force. For making solar evaporators, wood is cut horizontally to their growth direction to keep the internal microchannels intact for water transportation. Natural wood is an excellent heat insulator with very good thermal stability, making it suitable for designing different types of solar evaporators. Generally, two different approaches are observed in wood based solar evaporators, i) carbonizing wood substrate, and ii) loading wood substates with photothermal materials. Jia et al. [130] carbonised different types of wood, showed their performance in evaporating water, and concluded that reducing thickness may increase evaporation rate but decrease thermal confinement performance, leading to heat loss. Yu et al. [131] carbonized wood substrates of different thicknesses by hot plate carbonization technique and demonstrated that the thickness of 22 mm provides a maximum 6.90 kg m^{-2} h^{-1} evaporation rate under 5 sun. Kuang et al. [132] drilled natural wood blocks and carbonized their surface to make a solar evaporator which shows an efficiency of nearly 75% in highly concentrated (20 wt%) salt solution under OS. Jang et al. [133] utilized a CO_2 laser to make a graphitic carbon layer on the surface of basswood to make a solar evaporator that can be used in saline water for long-term operation. Xue et al. [134] used alcohol flame to carbonize wood, showing solar thermal efficiency of 72% under OS. Liu et al. [135] demonstrated a reverse-tree design by carbonising the surface of wood substrate obtained by cutting a natural tree parallel to the growth direction. Luo et al. [136] decorated wood substrates with different types of carbon based photothermal materials and shows their effectiveness in vapour generation. Ghafurian et al. [137] demonstrated different

wood surface treatment techniques (including gold coating) for making solar steam generators. Except that, many plasmonic metallic nanoparticles (i.e., Ag, Au, Pt, etc.) and semiconductor based photothermal material (e.g., $CuFeSe_2$, WO_{3-x} nanorod) deposited wood substrates have been reported for SSG [138-142]. Like wood substrate, some other bioderived solar evaporators (e.g., bamboo, jute stick) have also been reported where both carbonization technique and photothermal material deposition techniques were implied [143-145].

Polyurethane (PU) sponge is a porous substrate containing a path for water transport and has minimal thermal conductivity, making it suitable for designing solar evaporators and SSG devices.

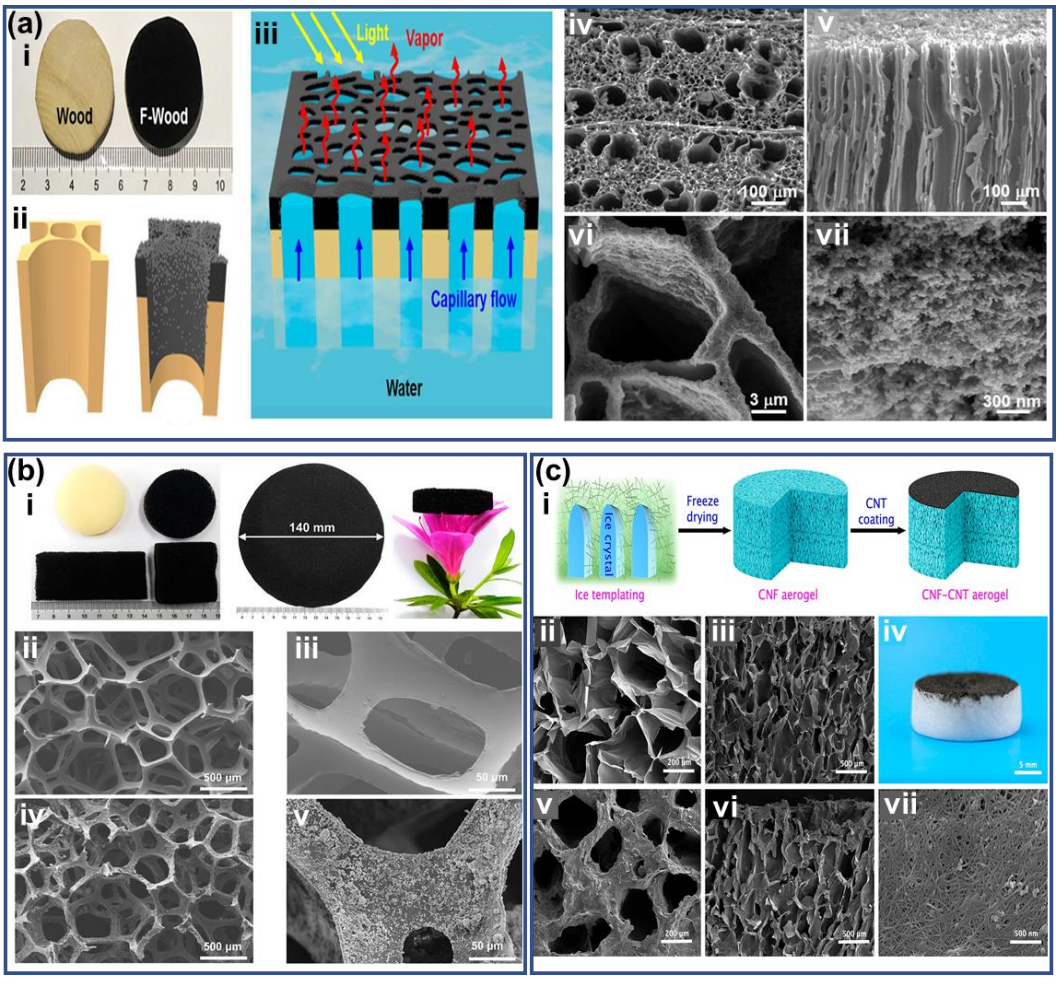

Figure 6. (a) (i-iii) Photograph and schematics of wood and flame treated wood, (iv-vi) SEM images of the top surface and cross section of flame treated wood and vii) morphology of deposited carbon nanoparticles [134], (b) (i) photograph of PU sponge and PACS. SEM images of (ii-iii) PU sponge (iv-v) PACS-120 [146], (c). i) schematics of the preparation process of CNF-CNT bilayer aerogel. SEM image showing the morphology of (ii-iii) CNF (v-vii) CNF-CNT aerogel and (iv) photograph of bilayer aerogel showing the layer of CNT coating on CNF aerogel [147].

Shi et al. [146] fabricated conjugated microporous polymer sponges by embedding porphyrin/aniline-based polymers on PU sponges by dip coating technique which shows sea water 1.33 kg m^{-2} h^{-1} evaporation rate and 87% PTC efficiency. Ivan et al. [148] fabricated a 3D solar evaporator and obtained a 1.4 kg m^{-2} h^{-1} evaporation rate and 79% PTC efficiency. The PU sponge acted as a support component to keep the evaporator floating on water and to facilitate faster water conveyance to the top surface of the absorber. Polydimethylsiloxane (PDMS) is a promising material for fabricating sponges for solar desalination for its high flexibility and thermal stability. Taking inspiration from the lotus leaf, Bu et al. [149] intricately designed a 3D evaporator that uses carbon fibre and cotton. The cone-shaped device features a conventional basket weaving method to provide adaptable water supply. By adjusting the quantity of water passages in the branches, it balances the water delivery and evaporation rate while maximising energy distribution on the carbon fibre surface. The 3D evaporator is highly effective in capturing sunlight and has an evaporation rate and photothermal conversion efficiency of 3.3 kg m^{-2} h^{-1} and 195% under one sun irradiation. The study delivers useful knowledge about the designing of SSG systems by illustrating how 3D structures can be optimized to ensure the harmonisation of water transport and evaporation, thus facilitating the production of energy efficient steam. However, the practical use of current solar evaporators is limited due to the

compromise between salt cycle and heat concentration. In order to overcome this problem, Liu et al. [150] developed a 3D solar evaporator that eliminates heat transfer from the evaporator to the bulk water while maintaining the water supply. They have achieved an evaporation rate of 2.3 kg m^{-2} h^{-1} and a solar to vapor efficiency of 137% under one sun condition. Wu et al. [151] created graphene-based evaporators for solar desalination of highly concentrated salt solutions (20 wt.% NaCl). The devices improve the evaporation rate and resistance to salt fouling, leading to their evaporator achieving a substantial evaporation rate of 2.6 kg m^{-2} h^{-1} during a one day test under one sun.

Cai et al. [152] derived a thermal responsive PDMS/CNT-PNIPAM sponge which shows a 1.7 kg m^{-2} h^{-1} evaporation rate under OS. Wang et al. [153] derived a 3D interpenetrating network sponge from natural polymer chitosan and gelatin for solar driven wastewater treatment. Except these, many other sponges (i.e., commercial sponge [154,155], carbon sponge [156], lignocellulose-based sponge [157], etc.) have been reported in the field of solar steam generation. Currently, nature-derived loofah sponge is also gaining attention for fabricating bio-derived solar evaporators due to its fibrous structure, low thermal conductivity and cost effectiveness [158,159]. Except for sponges, different types of foams have been reported for fabricating solar evaporators due to their microporous structure and chemical stability. Ren et al. [160] fabricated hierarchical graphene foam, which exhibits solar vapour conversion efficiency above 90% for seawater desalination. For low cost and strong structure, nickel foam [160] and copper foam [161] are widely used as supporting skeletons for photothermal materials. Monolithic polymer-based foam has also been fabricated or used as a substrate for making solar evaporators due to their various unique properties (e.g., mechanical strength, thermal stability, porous structure, chemical resistivity) [162-

164]. Chen et al. [164] showed the effectiveness (1.17 kg m^{-2} h^{-1} evaporation rate and 81% efficiency under OS) of fabricated polymer foam for SSG. Except for that bio-derived foam [165,166], melamine derived foam [167] is also used for designing 3D structured solar evaporators.

Different types of gels, i.e., hydrogel [168-170], and aerogels [147,171-175] are also used for fabricating solar evaporators for their hydrophilicity and porous structure. Moreover, aerogel has high mechanical strength, very low density, and thermal conductivity. The hydrophilic polymeric chain in hydrogel contains a polar functional group that creates a strong hydrogen bond with the water molecule and forms bound water. As this bond is strong, water molecules next to bound water interact with fewer water molecules and form intermediate water. Compared to bulk water, lower energy is needed for the intermediate water to escape from the liquid surface by breaking the hydrogen bond, which facilitates water evaporation [174,175]. Hydrogel and aerogel-based solar evaporators may give a higher evaporation rate. Gu et al. [175] fabricated an Integrated photothermal aerogel using chitosan, which shows a 1.80 kg m^{-2} h^{-1} evaporation rate under OS. Saleque et al. [176] fabricated a light trapping textured bio-hydrogel using agar-agar powder which shows an evaporation rate of 2.90 kg m^{-2} h^{-1} under OS.

4.3. Improving the water transport

The performance of the water transport channels or routes determines the efficiency of a solar evaporator. The water transport route greatly influences the efficiency of solar evaporators. In some cases, 3D evaporators, especially wood substrate-based 3D evaporators, are placed directly on water owing to the lower thermal conductivity of wood. For a heat localization system, thermal conductivity is a crucial parameter as

it determines the conductive heat loss from the absorber to bulk water. Depending on moisture content thermal conductivity of wood changes. For example, dry basswood's thermal conductivity can be 0.26 W m^{-1} K^{-1} whereas when it becomes wet, thermal conductivity reaches 0.47 W m^{-1} K^{-1} [133]. A similar change in thermal conductivity was reported for a flame treated wood (0.33 W m^{-1} K^{-1} for dry conditions and 0.55 W m^{-1} K^{-1} while loaded with water) [134]. However, the thermal conductivity in both cases is lower than in water (nearly around 0.6 W m^{-1} K^{-1}) [133,134,152]. Except for wood, sponge-based evaporators are sometimes kept on water directly due to their low thermal conductivity (0.644 W m^{-1} K^{-1}) [152]. Although these substrates (e.g., wood, sponge) have lower thermal conductivity, direct connection with water may cause heat loss by conduction from the absorber to feed water, reducing the efficiency of the solar evaporator [177]. Therefore, the concept of 1D and 2D water paths for water transportation has been developed, where the evaporator is kept separated from direct contact with bulk water by a heat insulator. In 1D water transportation system based solar evaporators, water is transported to the evaporator by a water transport route surrounded by a heat insulator. Generally, hydrophilic substances are used to make the 1D water transport route absorb and transport water faster. Nature shows the effectiveness of the 1D water transportation system through plants, where water is pumped by the route and supplied to the leaves by a confined path. Sun et al. [178] demonstrated a 3D structured carbonized sunflower head as a highly efficient evaporator (with an evaporation rate of 1.51 kg $m^{-2}h^{-1}$ under OS) where the stalk was utilized as a 1D channel. Xu et al. [179] made an evaporator by carbonising a mushroom and placing it on water with the help of a supporting foam, where the fibrous stripe act as a quasi-1D water transport route. Shi et al. [146] fabricated a solar evaporator (that obtained an evaporation rate of 2.31 kg m^{-2} h^{-1} under OS) by coating

carbon black nanoparticles on a flower like sponge and hydrophilic cotton strip as a 1D water transport route. Solar absorbers' 2D water transport route is generally made by surrounding a heat insulating body with a hydrophilic substance. Li et al. [180] wrapped a polystyrene foam (heat insulating body with thermal conductivity of nearly 0.04 W m^{-1} K^{-1}) by a thin layer of hydrophilic cellulose to construct a 2D water path for a graphene oxide based solar absorber, which shows the efficiency of nearly 80%. They have also demonstrated that the efficiency of the evaporator becomes low if the solar absorber is placed directly on water. Liu et al. [181] fitted a hat shaped foam with a cylindrical expanded polyethylene foam to create a 2D water transport path for the solar evaporator, which shows very good performance in desalinating sea water. Peng et al. [182] constructed a Janus evaporator with water transport channel by coating hydrophobic polyethylene wrapped cellulose aerogel by a hydrophobic soot-coated / hydrophilic cloth bilayer, which shows very good salt resisting capability while evaporating highly concentrated salt water.

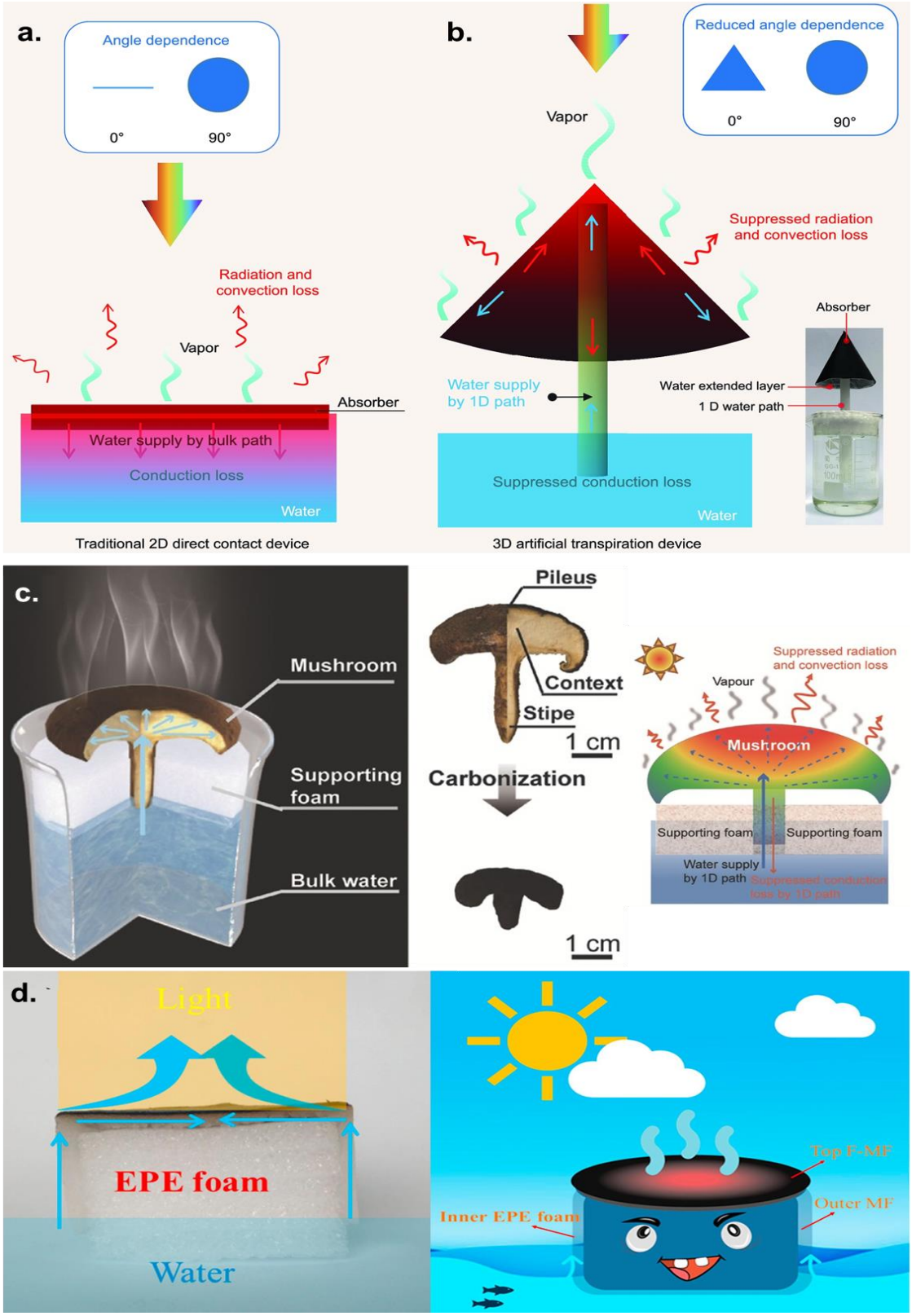

Figure 7. (a) Schematic of solar evaporator with direct water contact [180], (b) Schematic of artificial solar evaporator with 1D water transport path with the image of solar evaporator [180], (c) schematic of mushroom-based nature derived solar evaporator with 1D water transport system with the image of carbonised mushroom

[179], (d) Schematic illustration with the image of solar evaporator with 2D water path [181].

Zhang et al. [183] created a solar evaporator using a carbon black based nanofiber network with a 2D water path (made of microporous hydrophilic polyester) that shows an evaporation rate and PTC efficiency of 1.5 kg m^{-2} h^{-1} and 99% respectively. They have used PS foam as a support to keep the absorber floating on water surface and reduce thermal loss from the absorber to feed water. Except these, injection type water transport system [184-186] has also been reported where water is injected into the solar evaporator in a controlled way instead of sucking water from bulk water body for solar evaporation.

4.4. Salt resistance behaviour

Buildup of salt crystal on a top surface of a solar evaporator is one of the most challenging issues for desalinating seawater using interfacial SSG techniques. Salt crystal affects water transportation by blocking the water transport channels of the evaporator. Furthermore, when accumulated on the solar absorbing surface, the salt crystal reflects lights and reduces the evaporator's light absorbing behaviour. Therefore, the evaporation efficiency of solar evaporators reduces. Considering these issues, the researchers have proposed solar evaporators with different salt mitigation mechanisms [187]. Generally, during the evaporation experiment, in presence of light source, the sea or brine water starts to evaporate from the top surface of the evaporator. Therefore, salt concentration of water starts to increase at the top surface, and gradually, salt crystal starts to form. If the light source is removed, evaporation of water stops, and the salt begins to dissolve back into the buck water through the microchannels in the evaporator. The diameter of the microchannels as well as the

wettability of the evaporator, plays an important role in the case of self-cleaning. M. Zhu and co-workers fabricated plasmonic wood for solar evaporation application and showed this self-cleaning mechanism that depends on light availability [138]. According to this mechanism, if salt grows on evaporator's top surface, it will be cleaned automatically during night time when the evaporation rate of water is very low due to the absence of sunlight. Zhang et al. [183] reported a similar mechanism where within nearly 10 hours, all the accumulated salt was dissolved and removed from the evaporating surface due to the excellent absorption ability of CA/CB solar radiation. Generally, the naked eyes observe the salt cleaning process in such cases. To enhance the visibility of salt crystals, Ivan et al. [148] dried their solar evaporator using a drying oven after evaporating 10 wt% brine water solution and put it again on the 10 wt% brine water under no light condition. After 5 hours, no salt crystal was observed on the evaporator surface as the wastepaper derived egg tray-based solar evaporator dissolved the salt crystals.

Kuang et al. [132] came up with a new solution to stop salt growth during solar evaporation. They have drilled some arrays of holes in a wood substrate to create lateral salt gradients during evaporation. The wood substrate has natural microchannels with nearly 50 μm and nearly 12 μm diameter, whereas the drilled channels have a diameter of almost 1 mm. Therefore, when put on water, water in the channel was higher than in natural microchannels following fourth-power connection between the channel radius and flow through a capillary tube [188]. During the evaporation of sea water, the salt concentration in water becomes higher in the natural microchannels than in the drilled channels under the same light conditions, which creates lateral salt gradients. In the presence of natural pits on the walls of these channels, the lateral salt exchange occurs between drilled channels and natural

microchannels. It facilitates salts to return to bulk water by drilled channels of large diameters. This mechanism stopped the growth of salt during evaporating highly concentrated (20 wt%) brine water under OS and claimed to have remained stable over 100 h of continuous operation. A similar strategy was followed during the fabrication of evaporators by other researchers [189,190]. Drilled wood coated with Chinese ink shows no accretion of salt on the top surface after 2 h of evaporation of 4 wt% brine water under OS [190]. Ebrahimi et al. [191] exhibited that drilling channels on wood substrate can increase long term performance of solar evaporator (from 3 cycles to 11 cycles) under 3 sun as they help the natural micro channels of the wood substrate to reject salt by creating a lateral salt gradient.

Another most used strategy for stopping salt deposition on the surface of evaporator is to construct the evaporator with Janus characteristics. Generally, the Janus solar evaporators have two surfaces of two different properties, hydrophilic bottom surface for fast water absorption and hydrophobic top surface for solar absorption. In Janus solar evaporator, the evaporation of water takes place in hydrophobic–hydrophilic interface. Therefore, the thickness of hydrophobic solar absorbing surface should be kept low to shorten vapor escape route as well as heat conduction path [191]. Hydrophobic surface directly blocks the salt to be accumulated on solar absorbing surface and keeps highly salt concentrated water in hydrophobic-hydrophilic interface, while the hydrophilic bottom surface absorb huge amount of water which keeps the salt dissolved. Therefore, Janus evaporators shows excellent performance during long time operation [187]. Wang et al. [192] made-up flexible Janus solar evaporator and demonstrated that the Janus evaporator exhibits long term salt resistance while generating steam continuously for 7 days. Gu et al. [193] fabricated a solar evaporator with Janus based directional salt transfer structure which shows stable evaporation

rate of 1.22 kg m^{-2} h^{-1} using 10 wt% NaCl solution for 5 continuous days under OS. Tsang's group fabricated solar evaporators with natural holes from jute sticks and demonstrated the effect of hydrophilic and hydrophobic solar absorbing surface in rejecting salt [145]. The study demonstrated that though under OS hydrophilic absorbing surface offers an advanced sea water evaporation rate than hydrophobic solar absorbing surface; the salt rejection capability of hydrophobic surface is higher while evaporating highly salt concentrated water at higher solar intensity. Except for these Xia et al. [194] demonstrated a solar evaporator with controlled water transport property that facilitate edge preferential salt crystallization and gravity assisted salt collection. The fabricated evaporator shows almost no decline in water evaporation rate throughout 600 h of evaporation and salt collection. Later, Shao et al. [195] considered a bioinspired t-shaped mock tree following the concept of edge-preferential salt crystallization which shows a steady water evaporation rate of 2.03 kg m^{-2} h^{-1} for over 60 h with 75% PTC efficiency. Shi et al. [196] demonstrated a 3D cup shape design which can operate for at least 120 h without noticeable decay in water evaporation rate while evaporating 25 wt% salt concentrated water. Like the evaporators with edge-preferential salt crystallization capability, this 3D cup shape evaporator can also be used for harvesting salt as by product. A biomimetic cone shaped 3D structure was also demonstrated for solar evaporation and localized salt crystallization which can evaporate 25 wt% salt concentrated water at an evaporation rate of 2.63 kg $m^{-2}h^{-1}$ with PTC efficiency higher than 97% under OS [197].

Xia et al. [198] shown self-regenerating evaporator with self-rotating capability that exhibited high salt tolerance of 300 g/L and efficiency about 90%. The evaporator had the capability of removing salts from its top surface by rotating on water. Salt can also be rejected from the top surface of the evaporator using Marangoni flow [199-203].

Zou et al. [201] fabricated 3D bridge-arch evaporator to bring Marangoni flow by temperature gradient induced surface tension difference for rejecting salt and the evaporator shows long term salt rejecting capability while evaporating 10 wt% saline water for continuous 200 h. Shao et al. [202] reported that the crystallization of salt can be driven away from distillation zone using Marangoni effect and in their design the crystalized salt was accumulated outside the device during 36 h of continuous testing.

4.5. Corrosion resistance of the water transport layer

Except for salt, the presence of alkali or acidic substance in sea water or industrial water may reduce the lifetime of the solar evaporator by corrosion. Moreover, the growth of bacteria on the solar evaporator may also reduce the performance of the evaporator over time. Xu et al. [204] fabricated a solar evaporator using polyamide 6 graphene oxide membrane, which has high stability and strong acid and alkali corrosion resistance. Li et al. [205] utilized porous nickel mesh for fabricating a solar evaporator for its mechanical strength and corrosion resistance property which can remove substantial metal ions and dye molecules from polluted water. Sun et al. [206] fabricated a solar evaporator using 3D porous intermetallic compound as supporting material due to its resistance towards strong alkali, strong acid and salt spray corrosion.

The presence of micro-organism in sea water is another issue that may restrict the use of solar evaporators in real world application as some of these micro-organisms has the tendency to adhere to the evaporators [207]. The growth of these micro-organisms and their metabolites can reduce the performance of the solar evaporator by reducing their solar absorbing capability or by hampering their water transport

channels. Therefore, evaporators with anti-biofouling capability are proposed by many researchers. Generally, gram positive bacteria (i.e., S. aureus) and Gram-negative bacteria (i.e., E. coli) are cultured and utilised for showing the antibiofouling properties of the solar evaporator. The growth of bacteria in the presence of specific materials (used in solar evaporator) is observed to show the effectiveness of the materials in resisting bacterial growth. Wang et al. [208] utilized ZnO nano particles for fabricating solar steam device as ZnO nanocrystal can produce reactive oxygen species that can damage the bacterial cells and thus decrease bacterial growth. Xu et al. [209] demonstrated the effectiveness of CuO nanowire mesh in resisting the growth of *E. coli* as well as *S. aureus* and fabricated a solar evaporator with it that shows evaporation efficiency of 85% under OS. CuO mesh can release positive copper ions that can incorporate in negative cell membrane, leading to the escape of intracellular substances and cell death and hence it can be used to fabricate solar evaporators with anti-biofouling property. Tsang's group fabricated a bio-hydrogel for solar evaporation which shows its effectiveness against the growth of E. coli and S. aureus due to the presence of $TaTe_2$ quantum dots which have incredible kinship for sulfur proteins in bacterial DNA that can abolish the bacteria effectively and protect the solar evaporator from bacterial corrosion [176]. MXene based solar evaporator had also been reported for having antibiofouling property, where MXene layer itself worked as an extremely active bacteriostatic agent [210]. Except these many other solar evaporators have been fabricated that can provide resistance against bacterial corrosion [207, 211-213].

5. Enhancing desalination via condensation

The temperature difference between the water and the glass cover is crucial for the water produced and the efficiency of solar desalination. Plentiful approaches are

available to decrease the temperature in the condensation zone, such as glass cooling, external condensers, and thermoelectric cooling [214].

5.1. Glass cooling

In solar desalination systems, heat gained by evaporating water beneath the glass cover escapes to the surroundings through radiation and convection heat transfer. As convection heat transfer across the glass intensifies, the glass temperature drops, amplifying the temperature differential between the water and the glass cover. This temperature contrast drives a faster rate of water evaporation, leading to enhanced water production. The glass cover temperature can be lowered by implementing water flow, air flow, or a combination of both. Moreover, the flow of cooling water over the glass cover is crucial for enabling self-cleaning of the glass surface, ultimately maximizing solar radiation transmission through the glass cover.

Research on the cooling of glass to enhance condensation in solar desalination systems have shown a significant improvement in the productivity of water. Suneesh et al. [215] implemented a top cover for cooling, alongside airflow over the glass, resulting in a noteworthy increase in distillate production from 3300 to 4600 ml/m^2-day. Additionally, coating glass cover with silicone nanoparticles resulted in a remarkable 20% rise in water output [216]. The application of a flash tactic glass cover cooling technique showed an increase in the productivity of fresh water and the internal thermal efficiency [217]. Elmaadawy et al. [218] consistently achieved improved productivity using passive water-based glass cooling in comparison to conventional setups. A numerical model was used by Aghakhani et al. [219] to study the effect of glass-cooling on productivity of solar still. They implemented a selective water flow system that covered 10% of the glass and elevated performance by 28%. Hijleh [220]

analysed water film cooling and obtained 6% efficiency increase with optimised parameters. Samadony and Kabeel [221] researched the outcome of water cooling on solar stills, demonstrating an 8% increase in productivity that depended on specific parameter combinations. Khan et al. [222] increased the daily production of water in solar still by adding a water cooler. The final efficiency increased from 34% to 42%. Both of these studies demonstrate ways to improve the water productivity. Particular emphasis is placed on the role of cooling mechanisms in increasing distillate yield.

5.2. Thermoelectric cooling

Thermoelectric cooling effectively lowers the temperature of glass cooling water, enhancing condensation of water vapor and reducing the glass surface temperature, ultimately improving the water production efficiency of solar desalination systems.

Researchers investigated using thermoelectric cooling in solar desalination. In their study, Parsa et al. [223] found that the combination of thermoelectric cooling and water film cooling could contribute to approximately 26% of the total water production. Meanwhile, Manokar et al. [224] were able to increase freshwater production by 60% by employing thermoelectric cooling on the glass covering. Additionally, Khanmohammadi et al. [225] achieved a 30% increase in average freshwater production through continuous cooling of a double-glazed glass covering using a thermoelectric module. By introducing a condensation unit that sprays water onto the thermoelectric module, Colak et al. [226] improved water distillation, effectively speeding up the process. Shatar et al. [227] examined various thermoelectric cooling levels for a solar still with different cover materials, and found a remarkable 76% increase in productivity with a glass cover at 4 A current. Elgendi et al. [228] highlighted the dual cooling and heating capabilities of thermoelectric module in a solar still, with

the potential to increase condensation and evaporation, as well as generate electricity from thermal energy. Alwan et al. [229] improved condensation rates in a modified solar still by incorporating a thermoelectric cooling, resulting in 124% increased productivity compared to conventional stills. Rahbar et al. [230] developed a portable solar still that included a thermoelectric module and a heat-pipe cooling system. Their five day test demonstrated a consistently lower temperature than the walls, suggesting potential for higher water production. Dehghan et al. [231] constructed a thermodynamic model for a portable solar still that included a thermoelectric module. They found that the module was the main contributor to the exergy destruction, with the glass cover having the least effect. Esfe et al. [232] performed simulations to demonstrate that thermoelectric cooling uplifts water productivity by 7% in comparison to without cooling. Nazari et al. [233] experimented using solar still with an external thermoelectric condensation channel and found that the placement of four cooling modules around the channel walls increased still productivity by about 39%.

5.3. External condenser

The generated seam detaches from the absorber's surface and moves along the inner side of the glass cover due to natural convection and evaporative heat exchange between the absorber and the glass. By introducing forced convection heat transfer, water production increases as the condensation surface's temperature decreases. An external condenser, equipped with a fan, is employed to expedite water vapor removal and extract distilled water from the solar desalination system at the surrounding temperature. This process enhances the temperature contrast between the water and the condensation surface, as the ambient temperature remains lower than the inner glass temperature.

Toosi et al. [234] added an external condenser to their solar still, increasing productivity by 26% compared to the system without a condenser. Alawee et al. [235] discovered that, in their modified solar still, a suction fan conduces a significant percentage of water vapor towards an external condenser leading to a noteworthy increase of 120% in productivity. Abdullah et al. [236] carried out a comparative analysis of a conventional solar still and a modified solar still equipped with an external condenser. Water production was increased by approximately 57%, with the addition of an external condenser. In their investigations, Madhlopa and Johnstone [237] compared a solar still with a separate condenser against a conventional still, using numerical modeling. The modified design exhibited a 62% increase in distillate productivity. Samadony et al. [238] experimented with a modified stepped solar still, introducing reflectors, external condenser and fan to direct steam to a water-cooled heat exchanger. This setup led to a production increase of around 165% compared to a standard still. Zeroual et al. [239] enhanced a solar still's output by actively cooling the outer surface of the condenser using continuous water flow over the glass cover, yielding a 12% increase in productivity. In a comparative study, Hassan et al. [240] examined a solar still by comparing a conventional model with a glass liquefier to a model with a finned heatsink. During the summer, the heat sink condenser resulted in a 7% increase in freshwater yield along with a 12% boost in efficiency. The model featuring the plated finned heat sink condenser achieved a remarkable 42% efficiency. A study by Ibrahim et al. [241] investigated the effect of an external air-cooled condenser on the performance of a solar still and found a 16% increase in daily freshwater yield and a 30% improvement in energy efficiency compared to an unmodified still. Rabhi et al. [242] presented a modified solar still with a pin fin absorber and a condenser. The researchers discovered that utilising an external condenser,

alongside directing some humid air flow, led to a significant surge in water production. In comparison to a traditional still, the adapted version generated a remarkable 32% increase in water production. By adding reflectors and integrating a partial cooling coil condenser, Patel et al. [243] improved a double-slope solar still. The design allowed for primary condensation in a passive condenser connected to the still, which facilitated vapour transfer from the evaporation chamber. The inclusion of a partial cooling coil condenser enhanced vapor circulation between the chambers, significantly increasing the still's yield and efficiency. This segregated condensing surface greatly improved production, even in low solar radiation conditions. This makes it suitable for use in environments with limited sunlight.

6. Unlocking efficiency: strategies for efficient energy use

6.1. Efficient vapor generation

In SSG systems, the enthalpy of evaporation shows the energy needed to transform liquid into vapour at the interface of a solar absorbing material. Heat losses from thermal radiation, convection and conduction mean that not all the absorbed solar energy contributes to steam generation [54]. The thermal efficiency of evaporation denotes the successful use of heat for water evaporation generated from photothermal conversion. To achieve a high WP, it is essential to pursue a high thermal efficiency of evaporation, as prescribed by the SSG performance equation. Thus, it is crucial to implement effective thermal management strategies to minimize parasitic heat losses. A frequently used technique for thermal regulation involves reducing heat loss occurring between the absorber and water. Hydrophilic wicks are frequently used to transport water to the absorber, resulting in a successful outcome. An alternate approach is to utilize a thermal insulator possessing efficient capillary channels, which

is carefully situated between the absorber and the water, reducing the quantity of heat conducted to the bulk solution [186]. Another effective method of thermal management is the utilisation of a selective absorber, which can decrease thermal radiation losses to the atmosphere. When a non-selective blackbody absorber with high solar absorption is utilised, its emissivity is also high, leading to loss of heat through thermal radiation. This, in turn, decreases the amount of heat available for vapour generation [244].

6.2. Latent heat recovery

The standard for the evaluation of the WP in SSG systems characterises it as the amount of water that is produced per unit of solar radiation within a certain period of time. It establishes a correlation between WP and the effectiveness of utilising solar energy for steam generation and recovery of latent heat. Previous research in SSG systems has been aimed at improving the absorptivity of solar absorbers and the thermal efficiency of vapor generation, with a view to optimizing solar energy utilization. Given that current solar absorbers already achieve over 90% absorptivity, meaning that further improvements are limited. Therefore, future advancements in solar absorbing materials must to prioritise sustainability, cost reduction and environmental impact over merely maximising solar energy utilisation efficiency.

In a simple, solar steam generator system without heat recovery, accurate enclosure design is critical for effective steam condensation. Poor condensation can significantly impede the efficiency of solar energy utilization and nullify the benefits gained through rapid evaporation. The optimal approach to boost the WP of SSG systems lies in enhancing the GOR by executing efficient procedures for latent heat recovery. Although established thermal distillation technologies such as conventional multistage

flash and multiple effect distillation can achieve particularly high GORs (>15) [58]. Their performance tends to decline at smaller scales and usually requires significant investment. Therefore, it is crucial to develop simpler and more cost-effective approaches for the recovery of latent heat in order to significantly improve the GOR of small scale SSG systems.

6.3. Outlook

In SSG systems that use interfacial absorbers for direct steam generation, the design of the housing is crucial to overall performance beyond thermal management strategies. A well-designed housing fulfils two main criteria. Firstly, it must facilitate efficient vapour condensation to avoid saturation in the headspace, which could significantly reduce the driving force for water evaporation. Secondly, it should maintain the temperature required for water vapour generation by closely controlling the thermal energy input and output of the system. Future research should thoroughly evaluate how the housing design affects the productivity of SSG systems. In addition, this research should also guide the creation of economical enclosure solutions that function smoothly with high performance absorbers, ultimately enhancing the productivity.

7. Applications of interfacial steam generation

7.1. Saline water desalination

Interfacial SSG is getting attention in desalination as only about 3% of earth's water is fresh, and about 1.2% can be considered drinkable. Establishing conventional desalination systems requires high capital and operating costs due to high energy requirements. On the other hand, ISSG utilises solar energy for desalination. The electricity independent nature of ISSG makes it suitable for desalinating sea water and

purifying wastewater in many areas of the world where electricity is scarce. Therefore, in recent years ISSG techniques are mostly reported for desalinating saline water. ISSG procedure has also been reported for steam sterilization of medical equipment [245].

The presence of Na^+, K^+, Mg^{2+} and Ca^{2+} ions is widespread in seawater as it contains different types of salt. Generally, the concentration of these four ions is measured for purified water after solar desalination and compared with WHO (world health organization) standard for claiming the water is usable or drinkable. The quantity of ions is estimated by inductively coupled plasma mass spectroscopy. Lv et al. [246] measured the ions concentration of sea water (i.e., Na^+ = 14,614 mg/l, Mg^{2+} = 1370 mg/l, K^+ = 615 mg/l and Ca^{2+} = 620 mg/l) and demonstrated that the ion concentration becomes very low (Na^+ = 21.08 mg/l, Mg^{2+} = 6.88 mg/l, K^+ = 7.46 mg/l and Ca^{2+} = 9.72 mg/l) after condensing the vapour generated from evaporating sea water using 3D Janus radish based evaporator. Gu et al. [193] presented the concentration of major ions in sea water (Na^+ = 18,926.5 mg/l, Mg^{2+} = 1035.4 mg/l, K^+ = 709.3 mg/l and Ca^{2+} = 687.7 mg/l) as well as condensed water/ purified water (Na^+ = 8.4 mg/l, Mg^{2+} = 1.9 mg/l, K^+ = 3.8 mg/l and Ca^{2+} = 1.1 mg/l) and reported that the purified water meets the drinking water standard provided by WHO.

Sea water contains different types of salts; hence, the conductivity and salinity of seawater are higher. Hence, measuring the resistance, conductivity, and salinity can be another way to show water quality. Sun et al. [247] showed that the resistivity of desalinated water (1.5 MΩ) is higher than the water found from sea (0.19 MΩ) and from supply water (0.6 MΩ) of Dalian, China. Total dissolved solids (TDS) and hardness (amount of magnesium and calcium) are two essential factors in determining water quality. TDS determines the palatability, and according to WHO standards, the

TDS of water should be below 300 ppm for superb palatability [148]. Hard water or a high amount of magnesium and calcium can affect the supply line by scale deposition. Ivan et al. [148] measured the conductivity (μS/cm), salinity (%) and total dissolved solid (ppm) of condensed water (desalinated water), sea water, deionized water and supply water from Hong Kong using water quality tester EZ-9909 SP and reported that quality of purified water is better than sea water and supply water. TDS, conductivity, and salinity of sea water collected from Stanley, Hong Kong, 29,900 ppm, 48,900 μS/cm and 2.98%, respectively, and after solar evaporation and condensation TDS, conductivity and salinity of purified water turned out to be 31 ppm, 64 μS/cm and ≈ 0%.

7.2. Wastewater purification

An alternative exercise of interfacial SSG is purifying industrial wastewater. Different dye contaminated water is used as simulated industrial wastewater to demonstrate the effectiveness of solar evaporators in purifying wastewater. Generally, Methylene Blue (MB) [145,248], Methyl Orange (MO) [183], Rhodamine B (RhB) [248], Congo Red (CR) [145,204], Eriochrome Black T (EBT) [145], etc. are used for making simulated dye contaminated water. The UV-Vis absorption behaviour of dye contaminated water and purified water (found from condensing the vapour generated by evaporating dye wastewater) are observed to demonstrate the removal of dye from simulated wastewater. Except this, interfacial solar steam generation technique is also used for removal of heavy metal (e.g., Ni^{2+}, Cu^{2+}, Zn^{2+}, Pb^{2+}, Cd^{2+}, Hg^{2+}) [185,249] from simulated wastewater to demonstrate its effectiveness in purifying industrial wastewater and sewage water. Generally, an inductively coupled plasma mass spectrometer (ICP-MS, PQ-MS) is utilized to estimate ion concentration in simulated wastewater and purified water.

Zhang et al. [250] fabricated a vertical graphene film based solar absorber on producing clean water from polluted water. The effectiveness of MoS_2 based solar absorbers was studied by Chen et al. [251] to eliminate organic toxins through the photocatalytic oxidation method. In this study, the amount of carbon in specimens was examined both before and after the oxidation method, and outcomes showed that the amount decreased from 9.6 to 3.8 mg/L. They further also investigated actual saltwater samples. To treat industrial wastewater containing Cu^{2+} and MB, Deng et al. [252] synthesized a PVA sponge having a layer structure made of nano ink. After absorbing sunlight, the solar absorber materials produced highly reactive species, which reacted with organic toxins and broke down into minor, harmless molecules [209]. As heavy metals cannot be broken down, they can build up in living tissues and result in a number of illnesses and problems. They must therefore be removed before being discharged as effluent [253]. Zhu et al. [254] designed a solar absorbed using cotton cores and carbon black coated cellulose paper to decontaminate heavy metal and dye. They also claimed that including photocatalysis in the absorber may effectively degrade organic dye pollutants by photocatalysis. Li et al. [255] demonstrated solar steam generation efficiency (~100%) using MoS_2/C polyurethane sponge as well as efficiently removing the mercury from the wastewater. Zhu et al. [6] demonstrated a solar steam generation process for the application in the sterilization process.

Using solar vapour generation and photo-degradation, Hao et al. [256] demonstrated the ability to purify dye wastewater utilising TiO_2 polydopamine/PPy/cotton. Lin et al. [50] exhibited that using biochar, the solar steam generation process could enable faster response (approximately 9 mins) and more energy-efficient sterilisation than the traditional sterilisation methods. The acquired result shows that the pathogen has been effectively sterilized by almost 100%. Qu et al. [257] created a proof-of-principle

dwelling self-supply water arrangement to accomplish cyclic use of domestic sewage, such as wastewater from the dishwasher, dryer, and shower. Lou et al. [52] fabricated RGO-coated based paper for solar desalination as well as the purification of polluted water. The organic impurities in such composites can be eliminated in the RGO sheets thanks to the physical adsorption mechanism.

7.3. Energy generation

This section describes steam generation for use in energy applications. Two methods can generally be used to generate power from water evaporation. It has been extensively explored and demonstrated that solar energy might regenerate energy through photovoltaic, photoelectric, and photochemical processes [258,259]. To create fresh water and create electricity, it is usual practice to integrate evaporation tribo [28], piezo [29], thermoelectric [260], etc.

Li et al. [261] paired a thermoelectric segment with an evaporator to produce pure water and energy simultaneously. They reached 74% conversion efficiency as 1.4% thermoelectric conversion efficiency when temperature difference ranged from nearly 30 to 100°C. Using a ferroelectric fluoropolymer, polyvinylidene fluoride, Zhu et al. [262] demonstrated heat to electricity generation. The measured closed circuit current and open circuit voltage (V_{OC}) were nearly 80 nA, and 20 V. Yang et al. [263] presented a hybrid energy utilisation technology that simultaneously desalinated water and generated power via the difference in salinity due to evaporation. According to the findings, solar evaporation efficiency under a single sun may approach 75%, and an additional 1 W/m^2 of electric power could be generated. Ho's team also presented another hybrid system that produces power by condensation [28]. Water vapour-driven polymeric pyroelectric nanogenerators without any energy-guzzling alternating

devices were described by Gao et al. [264]. In this work, they observed V_{OC} of 145 V and a short circuit current of 0.12 A/cm^2. A CNT-based super hydrophilic filter paper was used as an absorber in their hybrid energy-generating technology presented by Yang et al. [265]. Under one sun, maximum efficiency of 76% was attained, and 1 W/m ^{2} of electrical output power was produced.

Zhu et al. [29] used polyvinylidene fluoride and ferroelectric fluoropolymer for energy generation. This study observed short-circuit current of 80 nA and V_{OC} of 20 V. In another study, Zhu et al. [266] employed a sponge on the absorber to increase output power density and heat localisation through its high broadband light-absorbing, heat-insulating properties. A maximum output power density was reached at 6.8 W m^{-2} under 5 sun. According to Zong et al. [267], nanofibril coated on thermal electricity can produce a Voc of 520 mV. Xue et al. [268] produced electricity using the water that evaporates from the surface of different carbon-based materials. In their study, evaporation from carbon black sheets (the size of a centimetre) can produce an open circuit voltage of 1 V in an ambient atmosphere. Zhang et al. [269] obtained an open circuit voltage of about 0.5 V using a pre-treated reduced graphene oxide-coated sponge. This strategy is considered a benchmark for developing energy harvesting, which can continuously produce electricity and evaporate water throughout the day and in any weather. Kral and Shapiro first put out the idea that flowing liquid through metallic SWNT causes electricity [270]. They claimed two mechanisms: momentum transfer from flowing liquid to carbon material and coulombic interaction between ionic /polar molecules in flowing liquid and carbon.

8. Challenges for solar-driven evaporation system

Despite recent advancements, there are still a number of significant obstacles that SSG technology must overcome.

- Currently, photothermal conversion efficiency is reached close to 100%. Therefore, it is essential to understand the exact calculation and how to tune different constraints for obtaining a superior water production rate. Moreover, it isn't easy to compare the performance of SSG systems as they operate under various experimental conditions. But it is crucial to substantiate the performance assessments of the SSG system under experimental conditions.
- There is a discontinuity between practical applications and the state-of-the-art of SSG system. To encourage acceptance by potential clients, low-cost, large-scale production must be developed. There have not yet been sufficient reports on the cost of PMs, structure, and system and their production scalability, which are obstacles to practical implementations. Estimating cost and scalability becomes newly viable for presenting research findings and the strategy for creating inexpensive materials and structures.
- Recent studies have largely concentrated on enhancing the rate of evaporation and carrying out long term stability assessments in saline water. However, the stability of the absorber under different harsh real-world conditions has not been given as much consideration. Stability of solar absorbers poses a major challenge in developing the SSG systems. To overcome this challenge, it is recommended that structural engineering techniques and the creation of absorbers with exceptional thermal stability in different environmental scenarios be investigated. However, it is important to note that the SSG uses real water sources that contain unstable organic compounds, which means that polluted

water is collected. It is therefore necessary for the absorber to be resistant to the pollutants and to be effective in the evaporation of the organic components.

- The dynamic kinetics of SSG presents a substantial design challenge for new materials and their structures. A comprehensive understanding of solar light absorption and conversion to thermal energy, water supply, heat loss and steam generation is essential for optimised material selection, structural arrangements and evaporation rates within the SSG system.
- Conduction, radiation, and convection are the three main types of heat diffusion in SSG system. While convection and radiation are infrequently investigated, considerable efforts in thermal diffusion are directed toward reducing thermal conduction. In addition to experimental data, modelling is a helpful tool for understanding fundamental kinetics and behaviours of processes connected to light, water, vapour, and heat.
- Almost all current efforts are directed toward creating steam during the day. However, SSG rate would alter with varying environmental factors like humidity, a wet day, etc. It might also decrease to a low value in a cloudy atmosphere. Hence, it is urgent to explore solar absorbers that can produce steam spontaneously in all weather conditions. To make this technology more accessible and have a brighter future, it is necessary to build SSG that can produce steam in any weather.

9. Conclusion and perspectives

Recently, much consideration has been remunerated to solar steam generation (SSG) as a low-cost, sustainable, renewable water supply and desalination option. The most recent SSG design and usage are reviewed in this study. Photothermal conversion is a sustainable and environmentally acceptable way of generating fresh water from

saltwater and dirty water. Various solar absorber materials and system design ideas have been highlighted to promote interfacial solar steam generation. We demonstrated how each idea improved solar absorptance and reduced heat losses, resulting in successful SSG. The absorber must be highly stable and recyclable to reduce financial and environmental costs. One approach to increase the impact of this research and innovation is through commercialization. As a result, a few scalable and valuable applications for energy production, wastewater purification, and saltwater desalination have emerged.

Despite the remarkable developments for SSG, a few problems still need to be resolved before this technology can be used in practical settings. However, there is a considerable disparity between laboratory scale and practical applications. Future work in this area should concentrate on

- There is a need to develop innovative structure photothermal material (PM). The creation of a multi-directional solar radiation-absorbing photothermal layer structure is necessary. This will improve light absorption while concentrating heat and allowing water to evaporate quickly, producing excellent water evaporation efficiency.
- Heat-to-vapor generation is tightly controlled by water movement and salt rejection. More research on the porosity, thickness, and dimensions of constructing structures with regulated features is necessary to explore the material's capacity for quick vapour release with salt rejection qualities.
- While lab scale solar steam generation efficiency has improved significantly, enhancing efficiency under real-world (practical) conditions is still a major challenge. The difference between lab conditions and practical use demands further refinement and optimization. For example, using SSG systems to treat

actual water sources poses significant pollution concerns. Extensive research is crucial to address the thermal stability, durability, consistency, water transportation, salt resistance, and long-term operational stability of SSG systems under particle-laden conditions.

- The photothermal mechanism has not been thoroughly studied. The thermodynamics of solar-driven evaporation have only seldom been studied in existing research, which is solely concerned with experimental data analysis and material selection. The following advancement of solar-driven evaporation can be facilitated by enlightenment for heat and mass transfer and impact of parameters like local heating and steam flow.
- The precise workings of the 3D absorber are still unclear, though. Thus, more extensive research on it is required. Additionally, more work should go into designing 3D structures, which have shown to be an excellent way to reduce heat loss and capture environmental energy, which could help improve system efficiency.
- It is essential to investigate further the stability and applicability of various SSG systems in acidic and basic ambient. In this review, stability and reusability are not sufficiently examined. In terms of practical techniques, there are significant research gaps.

References

1. T. Arunkumar, Yali Ao, Zhifang Luo, Lin Zhang, Jing Li, D. Denkenberger, J. Wang, 2019. Energy efficient materials for solar water distillation - A review, Renewable and Sustainable Energy Reviews, 115, 109409.
2. G. Ni, S.H. Zandavi, S.M. Javid, S.V. Boriskina, T.A. Cooper, G. Chen, 2018. A salt-rejecting floating solar still for low-cost desalination, Energy Environ. Sci., 11 1510 –1519.
3. L. Zhu, C. Fu Tan, M. Gao, G.W. Ho, 2015. Design of a Metal Oxide–Organic Framework (MoOF) Foam Microreactor: Solar-Induced Direct Pollutant Degradation and Hydrogen Generation, Adv. Mater., 27, 7713 –7719.
4. Mekonnen, M.M., Hoekstra, A.Y., 2016. Four billion people facing severe water scarcity, Sci. Adv. 2.
5. Arto, I., Andreoni, V., Rueda-Cantuche, J.M., 2016. Global use of water resources: a multiregional analysis of water use, water footprint and water trade balance. Water Res. Econo. 15, 1–14.
6. Li, J.L., Du, M.H., Lv, G.X., Zhou, L., Li, X.Q., Bertoluzzi, L., Liu, C.H., Zhu, S.N., Zhu, J., 2018a. Interfacial solar steam generation enables fast-responsive, energy-efficient, and low-cost off-grid sterilization. Adv. Mater. 30, 1805159.
7. R. Verbeke, V. Gómez, I.F.J. Vankelecom, 2017. Chlorine-resistance of reverse osmosis (RO) polyamide membranes, Prog. Polym. Sci., 72, 1 –15.
8. A.D. Khawaji, I.K. Kutubkhanah, J.-M. Wie, 2008. Advances in seawater desalination technologies, Desalination, 221, 47–69.
9. C. Chen, X. Zhao, L. Ye, 2022. Low Percolation Threshold and Enhanced Electromagnetic Interference Shielding in Polyoxymethylene/Carbon Nanotube

Nanocomposites with Conductive Segregated Networks, Ind. Eng. Chem. Res, 61, (11), 3962–3972.

10. L. Duan, Y. Zhou, H. Deng, X. Shi, Y. Chen, S. Zhang, Y. Hu, Q. Fu, 2019. The influence of blend composition and filer on the microstructure, crystallization, and mechanical behavior of polymer blends with multilayered structures, Nanocomposites, 4, (4), 178–189.
11. P. He, L. Hao, N. Liu, H. Bai, R. Niu, J. Gong, 2021. Controllable synthesis of sea urchinlike carbon from metal-organic frameworks for advanced solar vapor generators, Chem Eng J, 423, 130268.
12. R. Li, K. Shi, L. Ye, G. Li, 2019. Polyamide 6/graphene oxide-g-hindered phenol antioxidant nano-composites: Intercalation structure and synergistic thermal oxidative stabilization effect, Compos. B. Eng., 162, 11–20.
13. X. Ma, K. Chen, S. Li, Q. Huang, J. Zhu, J. Chen, N. Yan, 2022. Degradable Ti3C2TxMXene Nanosheets Containing a Lignin Polyurethane Photothermal Foam (LPUF) for Rapid Crude Oil Cleanup, ACS Appl. Nano Mater., 5 (2), 2848–2858.
14. L. Wang, Y. Feng, K. Wang, G. Liu, 2021. Solar water sterilization enabled by photothermal nanomaterials, NANO Energy, 87, 106158.
15. H. Zhou, C. Xue, Q. Chang, J. Yang, S. Hu, 2021. Assembling carbon dots on vertically aligned acetate fibers as ideal salt-rejecting evaporators for solar water purification, Chem Eng J, 421, 129822.
16. M. Gao, L. Zhu, C.K. Peh, G.W. Ho, 2019. Solar absorber material and system designs for photothermal water vaporization towards clean water and energy production, Energy Environ. Sci. 12, 841–864.

17. H.M. Qiblawey, 2008. F. Banat, Solar thermal desalination technologies, Desalination, 220, 633–644.
18. S.F. Anis, R. Hashaikeh, N. Hilal, 2019. Functional materials in desalination: a review, Desalination, 468, 114077.
19. Z. Wang, Y. Liu, P. Tao, Q. Shen, N. Yi, F. Zhang, Q. Liu, C. Song, D. Shang, T. Deng, 2014. Bio-inspired evaporation through plasmonic film of nanoparticles at the air-water interface, Small, 10, 3234–3239.
20. C. Chen, Y. Kuang, L. Hu, 2019. Challenges and opportunities for solar evaporation, Joule, 3, 683–718.
21. A. Kabeel, S. El-Agouz, 2011. Review of researches and developments on solar stills, Desalination, 276, 1–12.
22. Y. Zhang, M. Sivakumar, S. Yang, K. Enever, M. Ramezanianpour, 2018. Application of solar energy in water treatment processes: a review, Desalination, 428, 116–145.
23. L. Zhang, B. Tang, J. Wu, R. Li, P. Wang, 2015. Hydrophobic Light-to-Heat Conversion Membranes with Self-Healing Ability for Interfacial Solar Heating, Adv. Mater., 27, 4889–4894.
24. J. Zhou, Z. Sun, M. Chen, J. Wang, W. Qiao, D. Long, L. Ling, 2016. Macroscopic and Mechanically Robust Hollow Carbon Spheres with Superior Oil Adsorption and Light-to-Heat Evaporation Properties Adv. Funct. Mater., 26, 5368 –5375.
25. Z. Deng, J. Zhou, L. Miao, C. Liu, Y. Peng, L. Sun, S. Tanemura, 2017. The emergence of solar thermal utilization: solar-driven steam generation, J. Mater. Chem. A, 5, 7691 –7709.
26. W. Shang, T. Deng, 2016. Solar steam generation: Steam by thermal concentration, Nat. Energy, 1, 16133.

27. Y. Zhuang, L. Liu, X. Wu, Yu Tian, X. Zhou, S. Xu, Z. Xie, Y. Ma, 2019. Size and Shape Effect of Gold Nanoparticles in “Far-Field” Surface Plasmon Resonance, Part. Part. Syst. Charact., 36, 1800077.
28. M. Gao, C.K. Peh, H.T. Phan, L. Zhu, G.W. Ho, 2018. Solar Absorber Gel: Localized Macro-Nano Heat Channeling for Efficient Plasmonic Au Nanoflowers Photothermic Vaporization and Triboelectric Generation, Adv. Energy Mater., 8, 1800711.
29. L. Zhu, M. Gao, C.K.N. Peh, X. Wang, G.W. Ho, 2018. Self-Contained Monolithic Carbon Sponges for Solar-Driven Interfacial Water Evaporation Distillation and Electricity Generation, Adv. Energy Mater., 8, 1702149.
30. S. Karami, F. A. Roghabadi, M. Maleki, V. Ahmadi, S. M. Sadrameli, 2021. Materials and structures engineering of sun-light absorbers for efficient direct solar steam generation, Solar Energy, 225, 747–772.
31. A. Alsbaiee, B.J. Smith, L. Xiao, Y. Ling, D.E. Helbling, W.R. Dichtel, 2016. Rapid removal of organic micropollutants from water by a porous β-cyclodextrin polymer, Nature, 529, 190.
32. K.K. Liu, Q. Jiang, S. Tadepalli, R. Raliya, P. Biswas, R.R. Naik, S. Singamaneni, 2017. Wood-Graphene Oxide Composite for Highly Effiient Solar Steam Generation and Desalination, ACS Appl Mater Inter, 9 (8), 7675–7681.
33. H. Ren, M. Tang, B. Guan, K. Wang, J. Yang, F. Wang, M. Wang, J. Shan, Z. Chen, D.i. Wei, H. Peng, Z. Liu, 2017. Hierarchical Graphene Foam for Efficient Omnidirectional Solar-Thermal Energy Conversion, Adv Mater 29, (38), 1702590.
34. Qing Yin, Jingfa Zhang, Yubo Tao, Fangong Kong, Peng Li, 2022. The emerging development of solar evaporators in materials and structures, Chemosphere, 289, 133210.

35. H. Han, K. Huang, X. Meng, Review on solar-driven evaporator: development and applications, Journal of Industrial and Engineering Chemistry (2022), doi: https://doi.org/10.1016/j.jiec. 2022.11.051.
36. C. Chen, M. Wang, X. Chen, X. Chen, Q. Fu, H. Deng, 2022. Recent progress in solar photothermal steam technology for water purification and energy utilization, Chemical Engineering Journal, 448, 137603.
37. G. Liu, J. Xu, K. Wang, 2017. Solar water evaporation by black photothermal sheets Nano Energy 41, 269 –284.
38. L. Zhu, M. Gao, C.K.N. Peh, G.W. Ho, 2018. Solar-driven photothermal nanostructured materials designs and prerequisites for evaporation and catalysis applications, Mater. Horiz. 5, 323 –343.
39. S. Ishii, R.P. Sugavaneshwar, K. Chen, T.D. Dao, T. Nagao, 2016. Solar water heating and vaporization with silicon nanoparticles at mie resonances, Opt. Mater. Express 6, 640.
40. Z. Fang, Y.R Zhen, O. Neumann, A. Polman, F. Abajo, P. Nordlander, N. J. Halas, 2013. Evolution of Light-Induced Vapor Generation at a Liquid-Immersed Metallic Nanoparticle, Nano Lett., 13, 1736−1742.
41. A. Guo, Y. Fu, G. Wang, X. Wang, 2017. Diameter effect of gold nanoparticles on photothermal conversion for solar steam generation, RSC Adv., 7, 4815.
42. S.K. Hazra, S. Ghosh, T.K. Nandi, 2019. Photo-thermal conversion characteristics of carbon black-ethylene glycol nanofluids for applications in direct absorption solar collectors, Applied Thermal Engineering 163, 114402.
43. H. Ghasemi, G. Ni, A.M. Marconnet, J. Loomis, S. Yerci, N. Miljkovic, G. Chen, 2014. Solar steam generation by heat localization Nat. Commun. 5, 4449.

44. L. Zhu, M. Gao, C. Peh, G. Ho, 2019. Recent progress in solar-driven interfacial water evaporation: Advanced designs and applications, Nano Energy 57, 507–518.
45. T. Arunkumar, R. Jayaprakash, D. Denkenberger, A. Ahsan, M.S. Okundamiya, S. Kumar, H. Tanaka, H.S. Aybar, 2012. An experimental study on a hemispherical solar still Desalination 286, 342–348.
46. V.K. Dwivedi, G.N. Tiwari, 2010. Experimental validation of thermal model of a double slope active solar still under natural circulation mode, Desalination 250, 49–55.
47. J.T. Mahdi, B.E. Smith, A.O. Sharif, 2011. An experimental wick-type solar still system: Design and construction, Desalination 267, 233–238.
48. V. Sivakumar, E.G. Sundaram, 2013. Improvement techniques of solar still efficiency: A review, Renew. Sustain Energy Rev. 28, 246–264.
49. Y. Ito, Y. Tanabe, J. Han, T. Fujita, K. Tanigaki, M. Chen, 2015. Multifunctional Porous Graphene for High-Efficiency Steam Generation by Heat Localization, Adv. Mater. 27, 4302–4307.
50. X. Lin, J. Chen, Z. Yuan, M. Yang, G. Chen, D. Yu, M. Zhang, W. Hong, X. Chen, 2018. Integrative solar absorbers for highly efficient solar steam generation, J. Mater. Chem. A 6, 4642–4648.
51. Y. Liu, J. Chen, D. Guo, M. Cao, L. Jiang, 2015. Floatable, Self-Cleaning, and Carbon-Black-Based Superhydrophobic Gauze for the Solar Evaporation Enhancement at the Air−Water Interface, A.C.S. Appl, Mater. Inter. 7, 13645–13652.
52. J. Lou, Y. Liu, Z. Wang, D. Zhao, C. Song, J. Wu, N. Dasgupta, W. Zhang, D. Zhang, P. Tao, W. Shang, T. Deng, 2016. Bioinspired Multifunctional Paper-

Based rGO Composites for Solar Driven Clean Water Generation, A.C.S. Appl, Mater. Inter. 8, 14628–14636.

53. P. Zhang, Q. Liao, H. Yao, Y. Huang, H. Cheng, L. Qu, 2019. Direct solar steam generation system for clean water production, Energy Storage Materials 18, 429–446.
54. G. Ni, G. Li, S. Boriskina, H. Li, W. Yang, T. Zhang, G. Chen, 2016. Steam generation under one sun enabled by a floating structure with thermal concentration, Nat. Energy 1, 16126.
55. L. Zhou, Y. Tan, D. Ji, B. Zhu, P. Zhang, J. Xu, Q. Gan, Z. Yu, J. Zhu, 2016. Self-assembly of highly efficient, broadband plasmonic absorbers for solar steam generation. Sci. Adv. 2, e1501227.
56. M. Zhu, Y. Li, F. Chen, X. Zhu, J. Dai, Y. Li, Z. Yang, X. Yan, J. Song, Y. Wang, E. Hitz, W. Luo, M. Lu, B. Yang, L. Hu, 2018. Plasmonic wood for high-efficiency solar steam generation. Adv. Energy Mater. 8, 1701028.
57. R. L. McGinnis, M. Elimelech, 2007. Energy requirements of ammonia–carbon dioxide forward osmosis desalination. Desalination 207, 370–382.
58. Z. Wang, T. Horseman, A. P. Straub, N. Y. Yip, D. Li, M. Elimelech, S. Lin, 2019. Pathways and challenges for efficient solar-thermal desalination, Sci. Adv., 5:eaax0763.
59. X. Wu, G.Y. Chen, G. Owens, D. Chu, H. Xu, 2019. Photothermal materials: a key platform enabling highly efficient water evaporation driven by solar energy, Mater. Today Energy., 12, 277–296.
60. M. Gao, C.K. Peh, F.L. Meng, G.W. Ho, 2021. Photothermal membrane distillation toward solar water production, Small Methods.

61. Martinopoulos, G., Ikonomopoulos, A., Tsilingiridis, G., 2016. Initial evaluation of a phase change solar collector for desalination applications. Desalination 399, 165–170.

62. Liang, T., Fu, T., Hu, C., Chen, X., Su, S., Chen, J., 2021. Optimum matching of photovoltaic–thermophotovoltaic cells efficiently utilizing full-spectrum solar energy. Renew. Energy 173, 942–952.

63. A. Zeiny, H. Jin, L. Bai, G. Lin, D. Wen, 2018. A comparative study of direct absorption nanofluids for solar thermal applications, Solar Energy, 161, 74–82.

64. S. Jo, W. Lee, J. Park, H. Park, M. Kim, W. Kim, J. Hong, J. Park, 2021. Wide-range direct detection of 25-hydroxyvitamin D3 using polyethylene-glycol-free gold nanorod based on LSPR aptasensor, Biosensors and Bioelectronics, 181, 113118.

65. Chen, J., Ye, Z., Yang, F., Yin, Y., 2021b. Plasmonic Nanostructures for Photothermal Conversion, vol. 1, p. 2000055.

66. Fuku, K., Hayashi, R., Takakura, S., Kamegawa, T., Mori, K., Yamashita, H., 2013. The synthesis of size-and color-controlled silver nanoparticles by using microwave heating and their enhanced catalytic activity by localized surface plasmon resonance. Angew. Chem. Int. Ed. 52, 7446–7450.

67. Wang, M., Wang, P., Zhang, J., Li, C., Jin, Y., 2019. A ternary Pt/Au/TiO(2) - decorated plasmonic wood carbon for high-efficiency interfacial solar steam generation and photodegradation of tetracycline. ChemSusChem 12, 467–472.

68. A. Guo, Y. Fu, G. Wang, X. Wang, 2017. Diameter effect of gold nanoparticles on photothermal conversion for solar steam generation, RSC Adv., 7, 4815–4824.

69. Zhang, Q., Li, L., Jiang, B., Zhang, H.T., He, N., Yang, S., Tang, D., Song, Y.C., 2020d. Flexible and mildew-resistant wood-derived aerogel for stable and efficient solar desalination. ACS Appl. Mater. Interfaces 12, 28179–28187.

70. M. Chen, Y. He, J. Huang, J. Zhu, 2016. Synthesis and solar photo-thermal conversion of au, ag, and au-ag blended plasmonic nanoparticles, Energy Convers. Manag., 127, 293–300.

71. Zhu, H.W., Ge, J., Zhao, H.Y., Shi, L.A., Huang, J., Xu, L., Yu, S.H., 2020a. Sponge-templating synthesis of sandwich-like reduced graphene oxide nanoplates with confined gold nanoparticles and their enhanced stability for solar evaporation. Sci. China Mat. 63, 1957–1965.

72. Y. Lin, Z. Chen, L. Fang, M. Meng, Z. Liu, Y. Di, W. Cai, S. Huang, Z. Gan, 2018. Copper nanoparticles with near-unity, omnidirectional, and broadband optical absorption for highly effiient solar steam generation, Nanotechnology, 30, 0–11.

73. P. Fan, H. Wu, M. Zhong, H. Zhang, B. Bai, G. Jin, 2016. Large-scale cauliflower-shaped hierarchical copper nanostructures for efficient photothermal conversion, Nanoscale 8 14617–14624.

74. J. Xu, F. Xu, M. Qian, Z. Li, P. Sun, Z. Hong, F. Huang, 2018. Copper nanodot-embedded graphene urchins of nearly full-spectrum solar absorption and extraordinary solar desalination, Nano Energy, 53, 425–431.

75. M. Chen, Y. He, Q. Ye, X. Wang, Y. Hu, 2019. Shape-dependent solar thermal conversion properties of plasmonic au nanoparticles under different light filter conditions, Sol. Energy, 182, 340–347.

76. Zhou, L., Tan, Y.L., Wang, J.Y., Xu, W.C., Yuan, Y., Cai, W.S., Zhu, S.N., Zhu, J., 2016. 3D self-assembly of aluminium nanoparticles for plasmon-enhanced solar desalination. Nat. Photonics 10, 393.

77. Sun, Z.Y., Wang, J.J., Wu, Q.L., Wang, Z.Y., Wang, Z., Sun, J., Liu, C.J., 2019. Plasmon based double-layer hydrogel device for a highly effiient solar vapor generation. Adv. Funct. Mater. 29.

78. F. Tao, M. Green, A.V. Garcia, T. Xiao, A.T. Van Tran, Y. Zhang, Y. Yin, X. Chen, 2019. Recent progress of nanostructured interfacial solar vapor generators, Appl. Mater. Today, 17, 45–84.

79. L. Su, Y. Hu, Z. Ma, L. Miao, J. Zhou, Y. Ning, Z. Chang, B. Wu, M. Cao, R. Xia, J. Qian, 2020. Synthesis of hollow copper sulfied nanocubes with low emissivity for highly efficient solar steam generation, Sol. Energy Mater. Sol. Cells 210, 110484.

80. M. Sheikh, M. Pazirofteh, M. Dehghani, M. Asghari, M. Rezakazemi, C. Valderrama, J.L. Cortina, 2019. Application of ZnO nanostructures in ceramic and polymeric membranes for water and wastewater technologies: a review, Chem. Eng. J., 123475.

81. Wu, X., Robson, M.E., Phelps, J.L., Tan, J.S., Shao, B., Owens, G., Xu, H.L., 2019c. A flxible photothermal cotton-CuS nanocage-agarose aerogel towards portable solar steam generation. Nanomater. Energy 56, 708–715.

82. Wang, Z., Li, F., Shen, Z., Li, R., Zhang, X., Zhang, C., Wang, Y., Wang, Y., Zhang, H., Jian, X., Liu, J., Fan, C., 2021. Bi2S3/nylon membrane photothermal absorber with water shortage warning capability for seawater desalination. Mater. Lett. 286, 129188.

83. B.K. Tudu, V. Gupta, A. Kumar, A. Sinhamahapatra, 2020. Freshwater production via efficient oil-water separation and solar-assisted water evaporation using black titanium oxide nanoparticles, J. Colloid Interface Sci., 566, 183–193.

84. I. Zada, W. Zhang, P. Sun, M. Imtiaz, N. Iqbal, U. Ghani, R. Naz, Y. Zhang, Y. Li, J. Gu, Q. Liu, D. Pantelic, B. Jelenkovic, D. Zhang, 2020. Superior photothermal black TiO2 with random size distribution as flxible fim for effiient solar steam generation, Appl. Mater. Today, 20.

85. Ren, P., Li, J., Zhang, X., Yang, X., 2020. Highly efficient solar water evaporation of TiO2@TiN hyperbranched nanowires-carbonized wood hierarchical photothermal conversion material. Mat. Today Energy, 18.

86. M. Ye, J. Jia, Z. Wu, C. Qian, R. Chen, P.G. O'Brien, W. Sun, Y. Dong, G.A. Ozin, 2017. Synthesis of black TiOx nanoparticles by mg reduction of TiO2 nanocrystals and their application for solar water evaporation, Adv. Energy Mater., 7, 1–7.

87. Q. Wang, L. Qiu, Y. Jia, Y. Chang, X. Tan, L. Yang, H. Chen, 2019. Design of carbon loaded porous TiO2 foams by the hydrothermal-assisted annealing carbonization of fruit residue for solar-driven water evaporation, Sol. Energy Mater. Sol. Cells, 202, 110116.

88. Sun, Z., Li, Z., Li, W., Bian, F., 2020. Mesoporous cellulose/TiO2/SiO2/TiN-based nanocomposite hydrogels for efficient solar steam evaporation: low thermal conductivity and high light-heat conversion. Cellulose 27, 481–491.

89. Y. Zhang, K. Li, L. Liu, K. Wang, J. Xiang, D. Hou, J. Wang, 2020. Titanium nitride nanoparticle embedded membrane for photothermal membrane distillation, Chemosphere, 256, 127053.

90. Gao, M.M., Zhu, L.L., Peh, C.K., Ho, G.W., 2019. Solar absorber material and system designs for photothermal water vaporization towards clean water and energy production. Energy Environ. Sci., 12, 841–864.

91. Irshad, M.S., Arshad, N., Wang, X., 2021. Nanoenabled photothermal materials for clean water production. Global Challenges, 5, 2000055.

92. Velez-Cordero, J.R., Hernandez-Cordero, J., 2015. Heat generation and conduction in PDMS-carbon nanoparticle membranes irradiated with optical fibers. Int. J. Therm. Sci., 96, 12–22.

93. M. Rodrigues, J. Borges, C. Lopes, R. Pereira, M. Vasilevskiy, F. Vaz, 2021. Gas Sensors Based on Localized Surface Plasmon Resonances: Synthesis of Oxide Films with Embedded Metal Nanoparticles, Theory and Simulation, and Sensitivity Enhancement Strategies, Appl. Sci., 11, 5388.

94. A. Kumar, A. Kumar, V. Krishnan, 2020. Perovskite Oxide Based Materials for Energy and Environment-Oriented Photocatalysis, ACS Catal., 10, 10253 −10315.

95. X. Guo, H. Gao, L. Yin, S. Wang, Y. Dai, C. Feng, 2019. Photo-Thermal Conversion Materials and Their Application in Desalination, Progress in Chemistry, 31(4): 580-596.

96. X.Y. Wang, J. Xue, C. Ma, T. He, H. Qian, B. Wang, J. Liu, Y. Lu, 2019. Anti biofouling double-layered unidirectional scaffold for long-term solar-driven water evaporation, J. Mater. Chem., A 7, 16696–16703.

97. X. Hu, W. Xu, L. Zhou, Y. Tan, Y. Wang, S. Zhu, J. Zhu, 2017. Tailoring graphene oxide-based aerogels for efficient solar steam generation under one sun, Adv. Mater., 29.

98. G. Li, W.C. Law, K.C. Chan, 2018. Floating, highly efficient, and scalable graphene membranes for seawater desalination using solar energy, Green Chem., 20, 3689–3695.

99. Zhou, Q.X., Li, H., Li, D.D., Wang, B.B., Wang, H., Bai, J.B., Ma, S.H., Wang, G., 2021. A graphene assembled porous fiber-based Janus membrane for highly effective solar steam generation. J. Colloid Interface Sci., 592, 77–86.

100. K. Kim, S. Yu, C. An, S.W. Kim, J.H. Jang, 2018. Mesoporous three-dimensional graphene networks for highly efficient solar desalination under 1 sun illumination, ACS Appl. Mater. Interfaces, 10, 15602–15608.

101. Zhang, Z., Mu, P., He, J.X., Zhu, Z.Q., Sun, H.X., Wei, H.J., Liang, W.D., Li, A., 2019b. Facile and scalable fabrication of surface-modified sponge for efficient solar steam generation. ChemSusChem 12, 426–433.

102. Yang, J., Choi, J., Bang, D., Kim, E., Lim, E.K., Park, H., Suh, J.S., Lee, K., Yoo, K.H., Kim, E.K., Huh, Y.M., Haam, S., 2011. Convertible organic nanoparticles for near infrared photothermal ablation of cancer cells. Angew. Chem. Int., Ed. 50, 441–444.

103. X. Zhou, F. Zhao, Y. Guo, B. Rosenberger, G. Yu, 2019. Architecting highly hydratable polymer networks to tune the water state for solar water purification, Sci. Adv., 5.

104. Zou, Y., Yang, P., Yang, L., Li, N., Duan, G., Liu, X., Li, Y., 2021. Boosting solar steam generation by photothermal enhanced polydopamine/wood composites. Polymer 217, 123464.

105. X. Wu, G.Y. Chen, W. Zhang, X. Liu, H. Xu, 2017. A plant-transpiration-process inspired strategy for highly efficient solar evaporation, Adv. Sustain. Syst., 1, 1700046.

106. X. Zhao, X.J. Zha, L.S. Tang, J.H. Pu, K. Ke, R.Y. Bao, Z. Ying Liu, M.B. Yang, W. Yang, 2020. Self-assembled core-shell polydopamine@MXene with

synergistic solar absorption capability for highly efficient solar-to-vapor generation, Nano Res., 13, 255–264.

107. Huang, Q.C., Liang, X.C., Zhang, X.J., Yan, C.Y., Liang, J., Tang, H., Liu, Y.Z., 2021. Efficient-heat-utilization 3D T-shaped porous sponge assists 2D photothermal fims to achieve self-acting salt rejection and extra evaporation under high-concentration brine. Desalination, 499.
108. Fan, H.Q., Gao, A.L., Zhang, G.F., Zhao, S., Cui, J., Yan, Y.H., 2021. A design of bifunctional photothermal layer on polysulfone membrane with enclosed cellular-like structure for efficient solar steam generation. Chem. Eng. J., 415.
109. F. Tao, M. Green, A.V. Garcia, T. Xiao, A.T. Van Tran, Y. Zhang, Y. Yin, X. Chen, 2019. Recent progress of nanostructured interfacial solar vapor generators. Appl. Mater. Today., 17, 45–84.
110. H. Fan, A. Gao, G. Zhang, S. Zhao, J. Cui, Y. Yan, 2021. A design of bifunctional photothermal layer on polysulfone membrane with enclosed cellular-like structure for efficient solar steam generation, Chem. Eng. J., 415, 128798.
111. Y. Chang, Z. Wang, Y.E. Shi, X. Ma, L. Ma, Y. Zhang, J. Zhan, 2018. Hydrophobic W18O49 mesocrystal on hydrophilic PTFE membrane as an efficient solar steam generation device under one sun, J. Mater. Chem. A., 6, 10939–10946.
112. R. Du, H. Zhu, H. Zhao, H. Lu, C. Dong, M. Liu, F. Yang, J. Yang, J. Wang, J. Pan, 2023. Coupling ultrafine plasmonic Co3O4 with thin-layer carbon over SiO2 nanosphere for dual-functional PMS activation and solar interfacial water evaporation. Journal of Alloys and Compounds, 940, 168816.
113. G. Cheng, X. Wang, X. Liu, Y. He, B. V. Balakin, 2019. Enhanced interfacial solar steam generation with composite reduced graphene oxide membrane, Sol. Energy, 194, 415–430.

114. C.L. Guo, E.D. Miao, J.X. Zhao, L. Liang, Q. Liu, 2019. Paper-based integrated evaporation device for efficient solar steam generation through localized heating, Sol. Energy, 188, 1283–1291.

115. Q. Qi, Y. Wang, W. Wang, D. Yu, 2021. Surface self-assembled multi-layer MWCNTs-COOH/BN-PDA/CF for flexible and efficient solar steam generator, J. Clean. Prod., 279, 123626.

116. Y. Chen, S. Fang, L. Sun, F. Xu, M. Wang, J. Zhang, X. Mu, X. Wang, P. Wang, J. Liu, Z. Sun, H. Yao, J. Zhou, L. Miao, 2022. Hierarchical NiFe2O4-NiAl-LDH arrays immobilized on activated carbon cloth for bifunctional application on high-performance supercapacitors and solar steam generation, Sustain. Mater. Technol., 33, 00500.

117. Y. Li, X. Jin, Y. Zheng, W. Li, F. Zheng, W. Wang, T. Lin, Z. Zhu, 2019. Tunable Water Delivery in Carbon-Coated Fabrics for High-Efficiency Solar Vapor Generation, ACS Appl. Mater. Interfaces, 11, 46938–46946.

118. Q. Lu, Y. Yang, J. Feng, X. Wang, 2019. Oxygen-Defected Molybdenum Oxides Hierarchical Nanostructure Constructed by Atomic-Level Thickness Nanosheets as an Efficient Absorber for Solar Steam Generation, Sol. RRL, 3, 1–8.

119. L. Huang, J. Pei, H. Jiang, X. Hu, 2018. Water desalination under one sun using graphene-based material modified PTFE membrane, Desalination, 442, 1–7.

120. B. Bai, X. Yang, R. Tian, X.X. Wang, H. Wang, 2020. A high efficiency solar steam generation system with using residual heat to enhance steam escape, Desalination, 491, 114382.

121. H. Jiang, H. Fang, D. Wang, J. Sun, 2020. Spray-Coated Commercial PTFE Membrane from MoS 2 /LaF 3 /PDMS Ink as Solar Absorber for Efficient Solar Steam Generation, Sol. RRL, 4, 2000126.

122. N. Wei, Z. Li, Q. Li, E. Yang, R. Xu, X. Song, J. Sun, C. Dou, J. Tian, H. Cui, 2021. Scalable and low-cost fabrication of hydrophobic PVDF/WS2 porous membrane for highly efficient solar steam generation, J. Colloid Interface Sci., 588, 369–377.
123. M. Xia, J. Wei, Z. Han, Q. Tian, C. Xiao, Q.M. Hasi, Y. Zhang, L. Chen, 2022. An integrated solar absorber with salt-resistant and oleophobic based on PVDF composite membrane for solar steam generation, Mater. Today Energy, 25, 100959.
124. Z. Chen, J. Li, J. Zhou, X. Chen, 2023. Photothermal Janus PPy-SiO2@PAN/F-SiO2@PVDF-HFP membrane for high-efficient, low energy and stable desalination through solar membrane distillation, Chem. Eng. J., 451, 138473.
125. J. Huang, Y. Hu, Y. Bai, Y. He, J. Zhu, 2020. Novel solar membrane distillation enabled by a PDMS/CNT/PVDF membrane with localized heating, Desalination, 489, 114529.
126. A.A. Tessema, C.M. Wu, K.G. Motora, S. Naseem, 2021. Highly-efficient and salt-resistant CsxWO3@g-C3N4/PVDF fiber membranes for interfacial water evaporation, desalination, and sewage treatment, Compos. Sci. Technol., 211, 108865.
127. S. Gao, X. Dong, J. Huang, J. Dong, F. Di Maggio, S. Wang, F. Guo, T. Zhu, Z. Chen, Y. Lai, 2019. Bioinspired Soot-Deposited Janus Fabrics for Sustainable Solar Steam Generation with Salt-Rejection, Glob. Challenges, 3, 1800117.
128. Z. Qin, H. Sun, Y. Tang, S. Yin, L. Yang, M. Xu, Z. Liu, 2021. Bioinspired Hydrophilic–Hydrophobic Janus Composites for Highly Efficient Solar Steam Generation, ACS Appl. Mater. Interfaces., 13, 19467–19475.

129. X. Shan, A. Zhao, Y. Lin, Y. Hu, Y. Di, C. Liu, Z. Gan, 2020. Low-Cost, Scalable, and Reusable Photothermal Layers for Highly Efficient Solar Steam Generation and Versatile Energy Conversion, Adv. Sustain. Syst., 4, 1–8.
130. C. Jia, Y. Li, Z. Yang, G. Chen, Y. Yao, F. Jiang, Y. Kuang, G. Pastel, H. Xie, B. Yang, S. Das, L. Hu, 2017. Rich Mesostructures Derived from Natural Woods for Solar Steam Generation, Joule, 1, 588–599.
131. Z. Yu, S. Cheng, C. Li, Y. Sun, B. Li, 2019. Enhancing efficiency of carbonized wood based solar steam generator for wastewater treatment by optimizing the thickness, Sol. Energy, 193, 434–441.
132. Y. Kuang, C. Chen, S. He, E.M. Hitz, Y. Wang, W. Gan, R. Mi, L. Hu, 2019. A High-Performance Self-Regenerating Solar Evaporator for Continuous Water Desalination, Adv. Mater., 31, 1–8.
133. H. Jang, J. Choi, H. Lee, S. Jeon, 2020. Corrugated Wood Fabricated Using Laser-Induced Graphitization for Salt-Resistant Solar Steam Generation, ACS Appl. Mater. Interfaces, 12, 30320–30327.
134. G. Xue, K. Liu, Q. Chen, P. Yang, J. Li, T. Ding, J. Duan, B. Qi, J. Zhou, 2017. Robust and Low-Cost Flame-Treated Wood for High-Performance Solar Steam Generation, ACS Appl. Mater. Interfaces, 9, 15052–15057.
135. H. Liu, C. Chen, G. Chen, Y. Kuang, X. Zhao, J. Song, C. Jia, X. Xu, E. Hitz, H. Xie, S. Wang, F. Jiang, T. Li, Y. Li, A. Gong, R. Yang, S. Das, L. Hu, 2018. High-Performance Solar Steam Device with Layered Channels: Artificial Tree with a Reversed Design, Adv. Energy Mater., 8, 1–8.
136. X. Luo, C. Huang, S. Liu, J. Zhong, 2018. High performance of carbon-particle/bulk-wood bi-layer system for solar steam generation, Int. J. Energy Res., 42, 4830–4839.

137. M.M. Ghafurian, H. Niazmand, E. Ebrahimnia-Bajestan, R.A. Taylor, 2020. Wood surface treatment techniques for enhanced solar steam generation, Renewable Energy, 146, 2308-2315.
138. J. Wang, R. Wang, Y. Geng, Y. Li, J. Li, J. Qiu, M. Li, 2023. Activated pulverized coal membrane for effective solar-driven interfacial evaporation and desalination, Chem. Eng. Sci., 265, 118248.
139. R. Chen, K. Zhu, Q. Gan, Y. Yu, T. Zhang, X. Liu, M. Ye, Y. Yin, 2017. Interfacial solar heating by self-assembled Fe3O4@C film for steam generation, Mater. Chem. Front., 1, 2620–2626.
140. M. Zhu, Y. Li, F. Chen, X. Zhu, J. Dai, Y. Li, Z. Yang, X. Yan, J. Song, Y. Wang, E. Hitz, W. Luo, M. Lu, B. Yang, L. Hu, 2018. Plasmonic Wood for High-Efficiency Solar Steam Generation, Adv. Energy Mater., 8, 1701028.
141. K. Goharshadi, S.A. Sajjadi, E.K. Goharshadi, R. Mehrkhah, 2022. Highly efficient plasmonic wood/Ag/Pd photoabsorber in interfacial solar steam generation, Mater. Res. Bull., 154, 111916.
142. M. Wang, P. Wang, J. Zhang, C. Li, Y. Jin, 2019. A Ternary Pt/Au/TiO 2 - Decorated Plasmonic Wood Carbon for High-Efficiency Interfacial Solar Steam Generation and Photodegradation of Tetracycline, ChemSusChem., 12, 467–472.
143. H. Liu, C. Chen, H. Wen, R. Guo, N.A. Williams, B. Wang, F. Chen, L. Hu, 2018. Narrow bandgap semiconductor decorated wood membrane for high-efficiency solar-assisted water purification, J. Mater. Chem. A, 6, 18839–18846.
144. Z. Li, M. Zheng, N. Wei, Y. Lin, W. Chu, R. Xu, H. Wang, J. Tian, H. Cui, 2020. Broadband-absorbing WO3-x nanorod-decorated wood evaporator for highly

efficient solar-driven interfacial steam generation, Sol. Energy Mater. Sol. Cells, 205, 110254.

145. Y. Bian, Q. Du, K. Tang, Y. Shen, L. Hao, D. Zhou, X. Wang, Z. Xu, H. Zhang, L. Zhao, S. Zhu, J. Ye, H. Lu, Y. Yang, R. Zhang, Y. Zheng, S. Gu, 2019. Carbonized Bamboos as Excellent 3D Solar Vapor-Generation Devices, Adv. Mater. Technol., 4, 1–7.
146. Y. Shi, N. Meng, Y. Wang, Z. Cheng, W. Zhang, Y. Liao, 2022. Scalable Fabrication of Conjugated Microporous Polymer Sponges for Efficient Solar Steam Generation, ACS Appl. Mater. Interfaces, 14, 4522–4531.
147. C. Sheng, N. Yang, Y. Yan, X. Shen, C. Jin, Z. Wang, Q. Sun, 2020. Bamboo decorated with plasmonic nanoparticles for efficient solar steam generation, Appl. Therm. Eng., 167, 114712.
148. M.N.A.S. Ivan, A.M. Saleque, S. Ahmed, Z.L. Guo, D. Zu, L. Xu, T.I. Alam, S.U. Hani, Y.H. Tsang, 2023, Jute stick derived self-regenerating sustainable solar evaporators with different salt mitigation mechanisms for highly efficient solar desalination, J. Mater. Chem. A, 11, 3961.
149. Y. Bu, Y. Zhou, W. Lei, L. Ren, J. Xiao, H. Yang, W. Xu and J. Li, 2022. A bioinspired 3D solar evaporator with balanced water supply and evaporation for highly efficient photothermal steam generation, J. Mater. Chem. A, 10, 2856–2866.
150. H. Liu, B. Chen, Y. Chen, M. Zhou, F. Tian, Y. Li, J. Jiang, and W. Zhai, 2023. Bioinspired Self-Standing, Self-Floating 3D Solar Evaporators Breaking the Trade-Off between Salt Cycle and Heat Localization for Continuous Seawater Desalination, Adv. Mater., 35, 2301596.

151. S. Wu, S. Tian, R. Jian, L. Zhou, T. Luo, G. Xiong, 2023. Bio-inspired salt-fouling resistant graphene evaporators for solar desalination of hypersaline brines, Desalination, 546, 116197.

152. Y. Cai, Y. Dong, K. Wang, D. Tian, J. Qu, J. Hu, J. Lee, J. Li, K.H. Kim, 2023. A polydimethylsiloxane-based sponge for water purification and interfacial solar steam generation, J. Colloid Interface Sci., 629, 895–907.

153. X. Wang, Z. Li, Y. Wu, H. Guo, X. Zhang, Y. Yang, H. Mu, J. Duan, 2021. Construction of a Three-Dimensional Interpenetrating Network Sponge for High-Efficiency and Cavity-Enhanced Solar-Driven Wastewater Treatment, ACS Appl. Mater. Interfaces, 13, 10902–10915.

154. F. Jiang, H. Liu, Y. Li, Y. Kuang, X. Xu, C. Chen, H. Huang, C. Jia, X. Zhao, E. Hitz, Y. Zhou, R. Yang, L. Cui, L. Hu, 2018. Lightweight, Mesoporous, and Highly Absorptive All-Nanofiber Aerogel for Efficient Solar Steam Generation, ACS Appl. Mater. Interfaces, 10, 1104–1112.

155. M.N.A.S. Ivan, A.M. Saleque, S. Ahmed, P.K. Cheng, J. Qiao, T.I. Alam, Y.H. Tsang, 2022. Waste Egg Tray and Toner-Derived Highly Efficient 3D Solar Evaporator for Freshwater Generation, ACS Appl. Mater. Interfaces, 14, 7936−7948.

156. B. Shao, Y. Wang, X. Wu, Y. Lu, X. Yang, G.Y. Chen, G. Owens, H. Xu, 2020. Stackable nickel-cobalt@polydopamine nanosheet based photothermal sponges for highly efficient solar steam generation, J. Mater. Chem. A, 8, 11665–11673.

157. F. (Frank) Gong, H. Li, W. Wang, J. Huang, D. (David) Xia, J. Liao, M. Wu, D. V. Papavassiliou, 2019. Scalable, eco-friendly and ultrafast solar steam generators based on one-step melamine-derived carbon sponges toward water purification, Nano Energy, 58, 322–330.

158. H. Li, M. Yang, A. Chu, H. Yang, J. Chen, Z. Yang, Y. Qian, J. Fang, 2022. Sustainable Lignocellulose-Based Sponge Coated with Polypyrrole for Efficient Solar Steam Generation, ACS Appl. Polym. Mater, 4, 6572–6581.

159. A.M. Saleque, S. Ma, S. Ahmed, M.I. Hossain, W. Qarony, Y.H. Tsang, 2021. Solar Driven Interfacial Steam Generation Derived from Biodegradable Luffa Sponge, Adv. Sustain. Syst., 5, 2000291.

160. H. Ren, M. Tang, B. Guan, K. Wang, J. Yang, F. Wang, M. Wang, J. Shan, Z. Chen, D. Wei, H. Peng, Z. Liu, 2017. Hierarchical Graphene Foam for Efficient Omnidirectional Solar–Thermal Energy Conversion, Adv. Mater., 29, 1–7.

161. L. Ren, X. Yi, Z. Yang, D. Wang, L. Liu, J. Ye, 2021. Designing Carbonized Loofah Sponge Architectures with Plasmonic Cu Nanoparticles Encapsulated in Graphitic Layers for Highly Efficient Solar Vapor Generation, Nano Lett., 21, 1709–1715.

162. X. Shan, Y. Lin, A. Zhao, Y. Di, Y. Hu, Y. Guo, Z. Gan, 2019. Porous reduced graphene oxide/nickel foam for highly efficient solar steam generation, Nanotechnology, 30, 425403.

163. X. Gao, H. Ren, J. Zhou, R. Du, C. Yin, R. Liu, H. Peng, L. Tong, Z. Liu, J. Zhang, 2017. Synthesis of Hierarchical Graphdiyne-Based Architecture for Efficient Solar Steam Generation, Chem. Mater, 29, 5777–5781.

164. Q. Chen, Z. Pei, Y. Xu, Z. Li, Y. Yang, Y. Wei, Y. Ji, 2018. A durable monolithic polymer foam for efficient solar steam generation, Chem. Sci., 9, 623–628.

165. J. He, G. Zhao, P. Mu, H. Wei, Y. Su, H. Sun, Z. Zhu, W. Liang, A. Li, 2019. Scalable fabrication of monolithic porous foam based on cross-linked aromatic polymers for efficient solar steam generation, Solar Energy Materials and Solar Cells, 201, 110111.

166. J. He, Z. Zhang, C. Xiao, F. Liu, H. Sun, Z. Zhu, W. Liang, A. Li, 2020. High-Performance Salt-Rejecting and Cost-Effective Superhydrophilic Porous Monolithic Polymer Foam for Solar Steam Generation, ACS Appl. Mater. Interfaces, 12, 16308–16318.

167. C. Wang, J. Wang, Z. Li, K. Xu, T. Lei, W. Wang, 2020. Superhydrophilic porous carbon foam as a self-desalting monolithic solar steam generation device with high energy efficiency, J. Mater. Chem. A, 8, 9528–9535.

168. W. Fang, L. Zhao, X. He, H. Chen, W. Li, X. Zeng, X. Chen, Y. Shen, W. Zhang, 2020. Carbonized rice husk foam constructed by surfactant foaming method for solar steam generation, Renew. Energy, 151, 1067–1075.

169. W. Zhang, W. Zhu, S. Shi, N. Hu, Y. Suo, J. Wang, 2018. Bioinspired foam with large 3D macropores for efficient solar steam generation, J. Mater. Chem. A, 6, 16220–16227.

170. J. He, Y. Fan, C. Xiao, F. Liu, H. Sun, Z. Zhu, W. Liang, A. Li, 2021. Enhanced solar steam generation of hydrogel composite with aligned channel and shape memory behavior, Composites Science and Technology, 204, 108633.

171. N. Hu, Y. Xu, Z. Liu, M. Liu, X. Shao, J. Wang, 2020. Double-layer cellulose hydrogel solar steam generation for high-efficiency desalination, Carbohydrate Polymers, 243, 116480.

172. X. Yin, Y. Zhang, Q. Guo, X. Cai, J. Xiao, Z. Ding, J. Yang, 2018. Macroporous Double-Network Hydrogel for High-Efficiency Solar Steam Generation Under 1 sun Illumination, ACS Appl. Mater. Interfaces, 10, 10998–11007.

173. S. Han, T.P. Ruoko, J. Gladisch, J. Erlandsson, L. Wågberg, X. Crispin, S. Fabiano, 2020. Cellulose-Conducting Polymer Aerogels for Efficient Solar Steam Generation, Adv. Sustain. Syst., 4, 2000004.

174. X. Hu, W. Xu, L. Zhou, Y. Tan, Y. Wang, S. Zhu, J. Zhu, 2017. Tailoring Graphene Oxide-Based Aerogels for Efficient Solar Steam Generation under One Sun, Adv. Mater, 29, 1604031.

175. Y. Gu, X. Mu, P. Wang, X. Wang, J. Liu, J. Shi, A. Wei, Y. Tian, G. Zhu, H. Xu, J. Zhou, L. Miao, 2020. Integrated photothermal aerogels with ultrahigh-performance solar steam generation, Nano Energy, 74, 104857.

176. A. Mortuza Saleque, M. Nahian Al Subri Ivan, S. Ahmed, Y. Hong Tsang, 2023. Light-trapping Texture Bio-hydrogel with Anti-biofouling and Antibacterial Properties for Efficient Solar Desalination, Chemical Engineering Journal, 458, 141430.

177. X. Zhou, F. Zhao, Y. Guo, B. Rosenberger, G. Yu, 2019. Architecting highly hydratable polymer networks to tune the water state for solar water purification, Sci. Adv., 5, 1–8.

178. P. Sun, W. Zhang, I. Zada, Y. Zhang, J. Gu, Q. Liu, H. Su, D. Pantelić, B. Jelenković, D. Zhang, 2020. 3D-Structured Carbonized Sunflower Heads for Improved Energy Efficiency in Solar Steam Generation, ACS Appl. Mater. Interfaces, 12, 2171–2179.

179. N. Xu, X. Hu, W. Xu, X. Li, L. Zhou, S. Zhu, J. Zhu, 2017. Mushrooms as Efficient Solar Steam-Generation Devices, Adv. Mater., 29, 1–5.

180. X. Li, R. Lin, G. Ni, N. Xu, X. Hu, B. Zhu, G. Lv, J. Li, S. Zhu, J. Zhu, 2018. Three-dimensional artificial transpiration for efficient solar waste-water treatment, Natl. Sci. Rev., 5, 70–77.

181. P.F. Liu, L. Miao, Z. Deng, J. Zhou, Y. Gu, S. Chen, H. Cai, L. Sun, S. Tanemura, 2019. Flame-treated and fast-assembled foam system for direct solar steam

generation and non-plugging high salinity desalination with self-cleaning effect, Appl. Energy, 241, 652–659.

182. F. Peng, J. Xu, X. Bai, G. Feng, X. Zeng, M.R. Ibn Raihan, H. Bao, 2021. A janus solar evaporator with 2D water path for highly efficient salt-resisting solar steam generation, Sol. Energy Mater. Sol. Cells, 221, 110910.
183. R. Zhang, Y. Zhou, B. Xiang, X. Zeng, Y. Luo, X. Meng, S. Tang, 2021. Scalable Carbon Black Enhanced Nanofiber Network Films for High-Efficiency Solar Steam Generation, Adv. Mater. Interfaces, 8, 1–9.
184. F. Zhao, Y. Guo, X. Zhou, W. Shi, G. Yu, 2020. Materials for solar-powered water evaporation, Nat. Rev. Mater, 5, 388–401.
185. X. Min, B. Zhu, B. Li, J. Li, J. Zhu, 2021. Interfacial Solar Vapor Generation: Materials and Structural Design, Accounts Mater. Res., 2, 198–209.
186. X. Li, W. Xu, M. Tang, L. Zhou, B. Zhu, S. Zhu, J. Zhu, 2016. Graphene oxide-based efficient and scalable solar desalination under one sun with a confined 2D water path, Proc. Natl. Acad. Sci. U. S. A., 113, 13953–13958.
187. S. Liu, C. Huang, Q. Huang, F. Wang, C. Guo, 2019. A new carbon-black/cellulose-sponge system with water supplied by injection for enhancing solar vapor generation, J. Mater. Chem. A., 7, 17954–17965.
188. H. Liang, Q. Liao, N. Chen, Y. Liang, G. Lv, P. Zhang, B. Lu, L. Qu, 2019. Thermal Efficiency of Solar Steam Generation Approaching 100 % through Capillary Water Transport, Angew. Chemie Int. Ed., 58, 19041–19046.
189. K. Xu, C. Wang, Z. Li, S. Wu, J. Wang, 2021. Salt Mitigation Strategies of Solar-Driven Interfacial Desalination, Adv. Funct. Mater., 31, 2007855.

190. A.J. McElrone, W.T. Pockman, J. Martínez-Vilalta, R.B. Jackson, 2004. Variation in xylem structure and function in stems and roots of trees to 20 m depth, New Phytol., 163, 507–517.

191. A. Ebrahimi, E.K. Goharshadi, M. Mohammadi, 2022. Reduced graphene oxide/silver/wood as a salt-resistant photoabsorber in solar steam generation and a strong antibacterial agent, Mater. Chem. Phys., 275, 125258.

192. Q. Wang, L. Wang, S. Song, Y. Li, F. Jia, T. Feng, N. Hu, 2022. Flexible 2D@3D Janus evaporators for high-performance and continuous solar desalination, Desalination, 525, 115483.

193. R. Gu, Z. Yu, Y. Sun, P. Xie, Y. Li, S. Cheng, 2022. Enhancing stability of interfacial solar evaporator in high-salinity solutions by managing salt precipitation with Janus-based directional salt transfer structure, Desalination, 524, 115470.

194. Y. Xia, Q. Hou, H. Jubaer, Y. Li, Y. Kang, S. Yuan, H. Liu, M.W. Woo, L. Zhang, L. Gao, H. Wang, X. Zhang, 2019. Spatially isolating salt crystallisation from water evaporation for continuous solar steam generation and salt harvesting, Energy Environ. Sci., 12, 1840–1847.

195. Y. Shao, J. Tang, N. Li, T. Sun, L. Yang, D. Chen, H. Zhi, D. Wang, H. Liu, G. Xue, 2020. Designing a bioinspired synthetic tree by unidirectional freezing for simultaneous solar steam generation and salt collection, EcoMat., 2, 1–8.

196. Y. Shi, C. Zhang, R. Li, S. Zhuo, Y. Jin, L. Shi, S. Hong, J. Chang, C. Ong, P. Wang, 2018. Solar Evaporator with Controlled Salt Precipitation for Zero Liquid Discharge Desalination, Environ. Sci. Technol., 52, 11822–11830.

197. X. Zhang, Z. Wang, L. Song, Y. Feng, J. Yao, 2020. Chinese ink enabled wood evaporator for continuous water desalination, Desalination, 496, 114727.

198. Y. Xia, Y. Li, S. Yuan, Y. Kang, M. Jian, Q. Hou, L. Gao, H. Wang, X. Zhang, 2020. A self-rotating solar evaporator for continuous and efficient desalination of hypersaline brine, J. Mater. Chem. A, 8, 16212–16217.

199. Q. Zhang, G. Yi, Z. Fu, H. Yu, S. Chen, X. Quan, 2019. Vertically Aligned Janus MXene-Based Aerogels for Solar Desalination with High Efficiency and Salt Resistance, ACS Nano, 13, 13196–13207.

200. L. Wu, Z. Dong, Z. Cai, T. Ganapathy, N.X. Fang, C. Li, C. Yu, Y. Zhang, Y. Song, 2020. Highly efficient three-dimensional solar evaporator for high salinity desalination by localized crystallization, Nat. Commun., 11, 521.

201. M. Zou, Y. Zhang, Z. Cai, C. Li, Z. Sun, C. Yu, Z. Dong, L. Wu, Y. Song, 2021. 3D Printing a Biomimetic Bridge-Arch Solar Evaporator for Eliminating Salt Accumulation with Desalination and Agricultural Applications, Adv. Mater., 33, 2102443.

202. Y. Shao, A. Shen, N. Li, L. Yang, J. Tang, H. Zhi, D. Wang, G. Xue, 2022. Marangoni Effect Drives Salt Crystallization Away from the Distillation Zone for Large-Scale Continuous Solar Passive Desalination, ACS Appl. Mater. Interfaces, 14, 30324–30331.

203. M. Morciano, M. Fasano, S. V. Boriskina, E. Chiavazzo, P. Asinari, 2020. Solar passive distiller with high productivity and Marangoni effect-driven salt rejection, Energy Environ. Sci., 13, 3646–3655.

204. J. Xu, Y. Chen, M. Cao, C. Wang, P. Guo, 2022. Highly efficient solar steam generation of polyamide 6 membrane modified with graphene oxide and Au nanoparticles, J. Mater. Res., 37, 1475–1485.

205. Q. Li, S. Zhang, N. Wei, R. Xu, X. Li, L. Gong, H. Cui, 2022. Porous Ni/CNTs composite membrane as solar absorber for highly efficient solar steam generation, Sol. Energy Mater. Sol. Cells, 243, 111815.
206. K. Sun, H. Cui, R. Xu, L. Wang, M. Li, Z. Yang, M. Zhao, N. Wei, 2022. Constructing of 3D porous composite materials of NiAl/CNTs for highly efficient solar steam generation, Sol. Energy Mater. Sol. Cells, 240, 111722.
207. B. Peng, Q. Lyu, Y. Gao, M. Li, G. Xie, Z. Xie, H. Zhang, J. Ren, J. Zhu, L. Zhang, P. Wang, 2022. Composite Polyelectrolyte Photothermal Hydrogel with Anti-biofouling and Antibacterial Properties for the Real-World Application of Solar Steam Generation, ACS Appl. Mater. Interfaces, 14, 16546–16557.
208. X.Y. Wang, J. Xue, C. Ma, T. He, H. Qian, B. Wang, J. Liu, Y. Lu, 2019. Anti-biofouling double-layered unidirectional scaffold for long-term solar-driven water evaporation, J. Mater. Chem. A, 7, 16696–16703.
209. Y. Xu, J. Ma, Y. Han, J. Zhang, F. Cui, Y. Zhao, X. Li, W. Wang, 2019. Multifunctional CuO Nanowire Mesh for Highly Efficient Solar Evaporation and Water Purification, ACS Sustain. Chem. Eng., 7, 5476–5485.
210. X.J. Zha, X. Zhao, J.H. Pu, L.S. Tang, K. Ke, R.Y. Bao, L. Bai, Z.Y. Liu, M.B. Yang, W. Yang, 2019. Flexible Anti-Biofouling MXene/Cellulose Fibrous Membrane for Sustainable Solar-Driven Water Purification, ACS Appl. Mater. Interfaces, 11, 36589–36597.
211. Y. Xu, J. Ma, Y. Han, H. Xu, Y. Wang, D. Qi, W. Wang, 2020. A simple and universal strategy to deposit Ag/polypyrrole on various substrates for enhanced interfacial solar evaporation and antibacterial activity, Chem. Eng. J, 384, 123379.

212. L. Hao, N. Liu, H. Bai, P. He, R. Niu, J. Gong, 2022. High-performance solar-driven interfacial evaporation through molecular design of antibacterial, biomass-derived hydrogels, J. Colloid Interface Sci., 608, 840–852.
213. J. Yang, Y. Chen, X. Jia, Y. Li, S. Wang, H. Song, 2020. Wood-Based Solar Interface Evaporation Device with Self-Desalting and High Antibacterial Activity for Efficient Solar Steam Generation, ACS Appl. Mater. Interfaces, 12, 47029–47037.
214. S. Shoeibi, N. Rahbar, A. A. Esfahlani, H. Kargarsharifabad, 2021. A review of techniques for simultaneous enhancement of evaporation and condensation rates in solar stills, Solar Energy, 225, 666–693.
215. P.U. Suneesh, R. Jayaprakash, T. Arunkumar, D. Denkenberger, 2014. Effect of air flow on “V” type solar still with cotton gauze cooling, Desalination, 337, 1–5.
216. P. Zanganeh, A. S. Goharrizi, S. Ayatollahi, M. Feilizadeh, 2020. Nano-coated condensation surfaces enhanced the productivity of the single-slope solar still by changing the condensation mechanism, Journal of Cleaner Production, 265, 121758.
217. M.M. Morad, Hend A.M. El-Maghawry, Kamal I. Wasfy, 2015. Improving the double slope solar still performance by using flat-plate solar collector and cooling glass cover, Desalination, 373, 1–9.
218. K. Elmaadawy, A.W. Kandeal, A. Khalil, M.R. Elkadeem, B. Liu, S. W. Sharshir, 2021. Performance improvement of double slope solar still via combinations of low cost materials integrated with glass cooling, Desalination, 500, 114856.
219. H. Aghakhani, S.M. Ayatollahi, M.R. Hajmohammadi, 2023. Proposing novel approaches for solar still performance enhancement by basin water heating, glass cooling, and vacuum creation, Desalination, 567, 117011.

220. B. A. K. Abu-Hijleh, 1996. Enhanced solar still performance using water film cooling of the glass cover, Desalination, 107, 235-244.
221. Y. A . F. El-Samadony, A.E. Kabeel, 2014. Theoretical estimation of the optimum glass cover water film cooling parameters combinations of a stepped solar still, Energy, 68, 744-750.
222. M. Z. Khan, I. Nawaz, G.N. Tiwari, M. Meraj, 2021. Effect of top cover cooling on the performance of hemispherical solar still, Materials Today: Proceedings, 38, 384–390.
223. S. M. Parsa, A. Rahbar, M.H. Koleini, S. Aberoumand, M. Afrand, M. Amidpour, 2020. A renewable energy-driven thermoelectric-utilized solar still with external condenser loaded by silver/nanofluid for simultaneously water disinfection and desalination, Desalination, 480, 114354.
224. A. M.Manokar, M. Vimala, D. P.Winston, D.R. Rajendran, R. Sathyamurthy, A.E . Kabeel, 2020. Year around distilled water production, energy, and economic analysis of solar stills—A comparative study, Heat Transfer, 49, pp. 3651-3662.
225. S. Khanmohammadi, S. Khanjani, F. Musharavati, 2022. Experimental study and economic examination of double-glazed solar still desalination with a thermoelectric cooling system, Sustainable Energy Technologies and Assessments, 54, 102854.
226. A. Çolak, A. Çelik, E. Mandev, B. Muratçobanoglu, B. Gülmüs, F. Afshari, M. A. Ceviz, 2023. Study on a novel inclined solar water distillation system using thermoelectric module for condensation, Process Safety and Environmental Protection, 177, 986–994.

227. N. M. Shatar, M. F. M. Sabri, M. F. M. Salleh, M. H. Ani, 2023. Investigation on the performance of solar still with thermoelectric cooling system for various cover material, Renewable Energy, 202, 844–854.
228. M. Elgendi, A.E. Kabeel, F.A. Essa, 2023. Improving the solar still productivity using thermoelectric materials: A review, Alexandria Engineering Journal, 65, 963–982.
229. N. T. Alwan, A. S. Ahmed, M. H. Majeed, S. E. Shcheklein, S. J. Yaqoob, A. Nayyar, Y. Nam, and M. Abouhawwash, 2022. Enhancement of the Evaporation and Condensation Processes of a Solar Still with an Ultrasound Cotton Tent and a Thermoelectric Cooling Chamber, Electronics, 11, 284.
230. N. Rahbar, J.A. Esfahani, 2012. Experimental study of a novel portable solar still by utilizing the heatpipe and thermoelectric module, Desalination, 284, 55–61.
231. A. A. Dehghan, A. Afshari, N. Rahbar, 2015. Thermal modeling and exergetic analysis of a thermoelectric assisted solar still, Solar Energy, 115, 277–288.
232. M. H. Esfe, S. Esfandeh, D. Toghraie, 2021. Optimization of influential geometrical parameters of single slope solar still equipped with thermoelectric system to achieve maximum desalinated water, Energy Reports, 7, 5257–5268.
233. S. Nazari, H. Safarzadeh, M. Bahiraei, 2019. Experimental and analytical investigations of productivity, energy and exergy efficiency of a single slope solar still enhanced with thermoelectric channel and nanofluid, Renewable Energy, 135, 729-744.
234. S. S. A. Toosi, H. R. Goshayeshi, S. Z. Heris, 2021. Experimental investigation of stepped solar still with phase change material and external condenser, Journal of Energy Storage, 40, 102681.

235. W. H. Alawee, A.S. Abdullah, S. A. Mohammed, A. Majdi, Z.M. Omara, M.M. Younes, 2022. Testing a single slope solar still with copper heating coil, external condenser, and phase change material, Journal of Energy Storage, 56, 106030.
236. A.S. Abdullah, W. H. Alawee, S. A. Mohammed, Ali Majdi, Z.M. Omara, M.M. Younes, 2023. Utilizing a single slope solar still with copper heating coil, external condenser, phase change material, along with internal and external reflectors — Experimental study, Journal of Energy Storage, 63, 106899.
237. A. Madhlopa, C. Johnstone, 2009. Numerical study of a passive solar still with separate condenser, Renewable Energy, 34, 1668–1677.
238. Y. A. F. El-Samadony, A. S. Abdullah, and Z. M. Omara, 2015. Experimental study of stepped solar still integrated with reflectors and external condenser, Experimental Heat Transfer, 28:392–404.
239. M. Zeroual, H. Bouguettaia, D. Bechki, S. Boughalib, B. Bouchekima and H. Mahcene, 2011. Experimental investigation on a double-slope solar still with partially cooled condenser in the region of Ouargla (Algeria), Energy Procedia, 6, 736–742.
240. H. Hassan, M. S. Ahmed, M. Fathy, M. S. Yousef, 2020. Impact of salty water medium and condenser on the performance of single acting solar still incorporated with parabolic trough collector, Desalination, 480, 114324.
241. A. G. M. Ibrahim, E. E. Allam, S. E. Elshamarka, 2015. A modified basin type solar still: experimental performance and economic study, Energy, 93, 335–342.
242. K. Rabhi, R. Nciri, F. Nasri, C. Ali, H. B. Bacha, 2017. Experimental performance analysis of a modified single-basin single-slope solar still with pin fins absorber and condenser, Desalination, 416, 86–93.

243. S. K. Patel, D. Singh, G. L. Devnani, S. Sinha, D. Singh, 2021. Potable water production via desalination technique using solar still integrated with partial cooling coil condenser, Sustainable Energy Technologies and Assessments, 43, 100927.

244. F. E. Nicodemu, 1965. Directional reflectance and emissivity of an opaque surface. Appl. Optics, 4, 767–775.

245. A.M. Saleque, S. Ahmed, M.N.A.S. Ivan, M.I. Hossain, W. Qarony, P.K. Cheng, J. Qiao, Z.L. Guo, L. Zeng, Y.H. Tsang, 2022. High-temperature solar steam generation by MWCNT-HfTe2 van der Waals heterostructure for low-cost sterilization, Nano Energy, 94, 106916.

246. B. Lv, C. Gao, Y. Xu, X. Fan, J. Xiao, Y. Liu, C. Song, 2021. A self-floating, salt-resistant 3D Janus radish-based evaporator for highly efficient solar desalination, Desalination, 510, 115093.

247. Y. Sun, Z. Zhao, G. Zhao, L. Wang, D. Jia, Y. Yang, X. Liu, X. Wang, J. Qiu, 2021. High performance carbonized corncob-based 3D solar vapor steam generator enhanced by environmental energy, Carbon N. Y., 179, 337–347.

248. B. Yuan, C. Zhang, Y. Liang, L. Yang, H. Yang, L. Bai, D. Wei, W. Wang, Q. Wang, H. Chen, 2021. A Low-Cost 3D Spherical Evaporator with Unique Surface Topology and Inner Structure for Solar Water Evaporation-Assisted Dye Wastewater Treatment, Adv. Sustain. Syst., 5, 2000245.

249. Z. Ai, Y. Zhao, R. Gao, L. Chen, T. Wen, W. Wang, T. Zhang, W. Ge, S. Song, Self-assembly hierarchical binary gel based on MXene and montmorillonite nanosheets for efficient and stable solar steam generation, J. Clean. Prod. 357 (2022) 132000. https://doi.org/10.1016/j.jclepro.2022.132000.

250. P. Zhang, J. Li, L. Lv, Y. Zhao, L. Qu, 2017; Vertically Aligned Graphene Sheets Membrane for Highly Effiient Solar Thermal Generation of Clean Water, ACS Nano, 11 (5), 5087–5093.

251. R. Chen, X. Wang, Q. Gan, T. Zhang, K. Zhu, M. Ye, 2019; A bifunctional MoS2-based solar evaporator for both efficient water evaporation and clean freshwater collection, J. Mater. Chem. A, 7, 11177–11185.

252. Z. Deng, L. Miao, P.-F. Liu, J. Zhou, P. Wang, Y. Gu, X. Wang, H. Cai, L. Sun, S. Tanemura, 2019; Extremely high water-production created by a nanoink-stained PVA evaporator with embossment structure, NANO Energy, 55, 368–376.

253. W.W. Ngah, M.M. Hanafih, 2008; Removal of heavy metal ions from wastewater by chemically modifid plant wastes as adsorbents: a review, Bioresour. Technol. 99, 3935–3948.

254. X. Li, J. Li, J. Lu, N. Xu, C. Chen, X. Min, B. Zhu, H. Li, L. Zhou, S. Zhu, T. Zhang, J. Zhu, 2018; Enhancement of Interfacial Solar Vapor Generation by Environmental Energy, Joule 2, 1331–1338.

255. W. Li, M.C. Tekell, Y. Huang, K. Bertelsmann, M. Lau, D. Fan, 2018; Synergistic highrate solar steaming and mercury removal with MoS2/C@ polyurethane composite sponges, Adv. Energy Mater., 8, 1802108.

256. D. Hao, Y. Yang, Bi Xu, Z. Cai, 2018; Bifunctional Fabric with Photothermal Effect and Photocatalysis for Highly Effi cient Clean Water Generation, ACS Sustainable Chem. Eng., 6, 10789−10797.

257. P. Zhang, Q. Liao, H. Yao, H. Cheng, Y. Huang, C. Yang, L. Jiangc, L. Qu, 2018; Three-dimensional water evaporation on a macroporous vertically aligned graphene pillar array under one sun, J. Mater. Chem. A, 6, 15303.

258. Y. Lin, H. Xu, X. Shan, Y. Di, A. Zhao, Y. Hu, Z. Gan, 2019; Solar steam generation based on the photothermal effect: from designs to applications, and beyond, J Mater Chem A, 7 (33), 19203–19227.
259. I. Ihsanullah, 2020; Potential of MXenes in Water Desalination: Current Status and Perspectives, Nanomicro Lett, 12 (1), 72.
260. K. Liu, T. Ding, J. Li, Q. Chen, G. Xue, P. Yang, M. Xu, Z.L. Wang, J. Zhou, 2018, Thermal-Electric Nanogenerator Based on the Electrokinetic Effect in Porous Carbon Film, Adv Energy Mater, 8, 1702481.
261. X. Li, X. Min, J. Li, N. Xu, P. Zhu, B. Zhu, S. Zhu, J. Zhu, 2018, Storage and Recycling of Interfacial Solar Steam Enthalpy Joule, 2 (11), 2477–2484.
262. L. Zhu, M. Gao, C. K. N. Peh, X. Wang, G. W. Ho, 2018, Self-Contained Monolithic Carbon Sponges for Solar-Driven Interfacial Water Evaporation Distillation and Electricity Generation, Adv. Energy Mater., 8, 1702149.
263. P. Yang, K. Liu, Q. Chen, J. Li, J. Duan, G. Xue, Z. Xu, W. Xie, J. Zhou, 2017, Solar driven simultaneous steam production and electricity generation from salinity, Energy Environ Sci, 10 (9), 1923–1927.
264. F. Gao, W. Li, X. Wang, X. Fang, M. Ma, 2016, A self-sustaining pyroelectric nanogenerator driven by water vapor, Nano Energy, 22, 19–26.
265. P. Yang, K. Liu, Q. Chen, J. Li, J. Duan, G. Xue, Z. Xu, W. Xie, J. Zhou, 2017, Solar-driven simultaneous steam production and electricity generation from salinity, Energy Environ. Sci., 10, 1923 –1927.
266. L. Zhu, T. Ding, M. Gao, C.K.N. Peh, G.W. Ho, 2019, Shape conformal and thermal insulative organic solar absorber sponge for photothermal water evaporation and thermoelectric power generation, Adv. Energy Mater., 9, 1900250.

267. L. Zong, M. Li, C. Li, 2018, Intensifying solar-thermal harvest of low-dimension biologic nanostructures for electric power and solar desalination, Nano Energy, 50, 308–315.

268. G. Xue, Y. Xu, T. Ding, J. Li, J. Yin, W. Fei, Y. Cao, J. Yu, L. Yuan, L. Gong, J. Chen, S. Deng, J. Zhou, W. Guo, 2017, Water-evaporation-induced electricity with nanostructured carbon materials, Nat. Nanotechnol. 12, 317.

269. G. Zhang, Z. Duan, X. Qi, Y. Xu, L. Li, W. Ma, H. Zhang, C. Liu, W. Yao, 2019, Harvesting environment energy from water-evaporation over free-standing graphene oxide sponges, Carbon, 148,1–8.

270. P. Kral, M. Shapiro, 2001, Nanotube electron drag in flowing liquids, Phys. Rev. Lett., 86, 131.